
Loss Landscape of Shallow ReLU-like Neural Networks: Stationary Points, Saddle Escaping, and Network Embedding

Zhengqing Wu
EPFL, Switzerland
zhengqing.wu@epfl.ch

Berfin Şimşek
New York University, USA
bs3736@nyu.edu

François Ged
EPFL, Switzerland
francois.ged@epfl.ch

Abstract

In this paper, we investigate the loss landscape of one-hidden-layer neural networks with ReLU-like activation functions trained with the empirical squared loss. As the activation function is non-differentiable, it is so far unclear how to completely characterize the stationary points. We propose the conditions for stationarity that apply to both non-differentiable and differentiable cases. Additionally, we show that, if a stationary point does not contain "escape neurons", which are defined with first-order conditions, then it must be a local minimum. Moreover, for the scalar-output case, the presence of an escape neuron guarantees that the stationary point is not a local minimum. Our results refine the description of the *saddle-to-saddle* training process starting from infinitesimally small (vanishing) initialization for shallow ReLU-like networks, linking saddle escaping directly with the parameter changes of escape neurons. Moreover, we are also able to fully discuss how network embedding, which is to instantiate a narrower network within a wider network, reshapes the stationary points.

1 Introduction

Understanding the training process of neural networks calls for insights into their loss landscapes. Characterization of the stationary points is a crucial aspect of these studies. In this paper, we investigate the stationary points of the loss of a one-hidden-layer neural network with activation functions that are ReLU-like. The non-differentiability of the activation function renders such problems non-trivial. It is worth noting that, although the non-differentiable areas only account for zero Lebesgue measure in the parameter space, such areas are often visited by gradient flow and thus should not be neglected.

In particular, when the network output is unidimensional, we identify the "escape neuron", which prevents a stationary point from being a local minimum. It allows for an escape direction that enables the training to further toward a better approximation of the training data. Empirically, we observe that the training trajectory might get stuck at a local minimum, which we are able to identify by the absence of an escape neuron. Our results provide insight into the saddle escaping process with minimal assumptions. Firstly, we do not require the hidden layer to be infinitely wide as in [1–3]. Moreover, we extend the discussion by [4, 5] and [6, 7]. The former two require strong assumptions on the training inputs, and the latter two study the process before the parameters leave the first saddle.

We are also able to systematically describe how network embedding reshapes the stationary points by examining whether the "escape neurons" are generated from the embedding process. This directly supplements the discussion by [8] for the non-differentiable cases.

1.1 Related Work

Stationary Points. Stationary points abound in neural network loss functions. It has been shown that there exists a plethora of saddle points and spurious local minima for non-linear networks [9–13]. Additionally, stationary points may significantly affect the training dynamics, resulting in plateaus in training loss [14–17]. When studying these stationary points, it is of both theoretical and practical interest [18, 19] to discriminate between their different types [20], for they affect gradient descent (GD) differently [21, 22]. For example, while local minima and non-strict saddles are not escapable [20, 22, 23], strict saddles are mostly escapable under mild conditions [21, 22, 24–26]. In our setting, the non-differentiability complicates the analysis. To tame such difficulty, previous works took various simplifications, such as only studying the differentiable areas [9, 27, 28], only studying parameters with zero right-hand derivatives [29], and only studying non-differentiable stationary points yielded by restrictive constructions [11]. The resulting theories failed to cover all the cases due to such simplifications. So far, a systematic characterization of the potentially non-differentiable stationary points in our setting is yet to be established.

Training Dynamics. Different initialization scales lead to different training dynamics. In the lazy-training regime [2], which has relatively large initialization scales, the dynamics is well captured by the neural tangent kernel theory [1, 3, 30]. In the regime of vanishing initialization, the training displays a feature learning behavior [31]. A generic theory for such dynamics is still missing. However, it has been widely observed that the training dynamics in this regime often assumes a saddle-to-saddle pattern [4, 5, 16, 17, 32], meaning the loss will experience intermittent steep declines punctuated by plateaus where it remains relatively unchanged. We will describe this process for our setting, furthering the discussions from [4–7]. It is noteworthy that the training dynamics often unveils the implicit biases induced by vanishing initialization. In the saddle-to-saddle regime, the learned functions often prefer lower parameter ranks [6, 16, 33] or smaller parameter norms [4, 17], which could be beneficial for generalization.

Network Embedding. Network embedding provides a perspective for understanding how the optimization landscape transforms given more parameters. This can shed light on the merit of over-parameterization, a widely studied topic [34–41]. Previously, network embedding has been studied in various setups [8, 18, 19, 32, 42], mostly focusing on how network embedding reshapes stationary points. We extend this line of work to the cases where non-differentiability is involved.

1.2 Main Contribution

In this paper, we study the aforementioned topics for one-hidden-layer networks with ReLU-like activation functions, the loss being empirical squared loss. We make minimal assumptions and achieve the following.

- Noticing that the non-differentiability only lies within hyper-planes orthogonal to training inputs, and derivatives can be handled easily on both sides of those hyperplanes, we develop a routine to methodically and fully investigate the directional derivative of the loss. With its help, we identify and characterize different types of stationary points with non-differentiability fully considered.
- We show that saddle escaping must involve the parameter changes of escape neurons (Definition 4.1). We apply this to the description of the training dynamics with vanishing initialization.
- We study whether network embedding preserves stationarity or local minimality.

2 Setup

Network Architecture. We study one-hidden-layer networks as illustrated in Figure 1.

For a given input $\mathbf{x} \in \mathbb{R}^d$, the network output is:

$$\hat{\mathbf{y}}(H, W; \mathbf{x}) = \hat{\mathbf{y}}(\mathbf{P}; \mathbf{x}) = H\rho(W\mathbf{x}). \quad (1)$$

In Equation (1), $W \in \mathbb{R}^{|I| \times d}$ and $H = (h_{ji}) \in \mathbb{R}^{|J| \times |I|}$ are respectively the input and output weight matrices, and

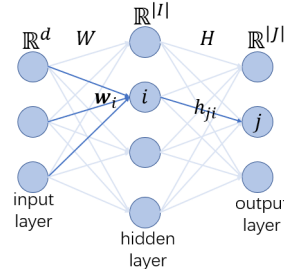


Figure 1: Network Architecture.

I and J are the sets of indices of the hidden neurons and output neurons. The vector $\mathbf{P} \in \mathbb{R}^D$ contains all the trainable parameters W and H , so that $D = |J| \times |I| + |I| \times d$. We denote the row of W corresponding to hidden neuron i by $\mathbf{w}_i \in \mathbb{R}^d$. The componentwise activation function $\rho(\cdot)$ reads:

$$\rho(z) = \alpha^+ \mathbb{1}_{z \geq 0} z + \alpha^- \mathbb{1}_{z < 0} z; \quad \alpha^+, \alpha^-, z \in \mathbb{R}.$$

In this paper, the *assumptions* we make are $\alpha^+ \neq \alpha^-$ and $d > 1$. Both are for the sake of brevity in exposition, rather than being indispensable for the validity of the outcomes.

Loss Function. The training input/targets are $\mathbf{x}_k/\mathbf{y}_k$ with $k \in K$, where K denotes the set containing the sample indices. The empirical squared loss function takes the form:

$$\mathcal{L}(\mathbf{P}) = \frac{1}{2} \sum_{k \in K} \|\hat{\mathbf{y}}_k(\mathbf{P}) - \mathbf{y}_k\|^2 = \frac{1}{2} \sum_{j \in J} \sum_{k \in K} (\hat{y}_{kj}(\mathbf{P}) - y_{kj})^2, \quad (2)$$

where $\hat{\mathbf{y}}_k(\mathbf{P}) := \hat{\mathbf{y}}(\mathbf{P}; \mathbf{x}_k)$, and \hat{y}_{kj}, y_{kj} are the components of $\hat{\mathbf{y}}_k$ and \mathbf{y}_k at the output neuron j .

3 Basics

In this section, we derive the first-order derivatives and identify stationary points of the loss.

3.1 First-order Derivatives of the Loss

We start by introducing a suitable coordinate system on which the first-order directional derivatives of the loss are well-defined and computable.

Non-differentiability does not completely prohibit the investigation into derivatives. Take the function, $f(x) = |x|$, as a pedagogical example. In this case, studying the left and right derivatives at $x = 0$ suffices to describe the function locally, despite the non-differentiability there. Generalizing this methodology to higher dimensions, we can handle the derivatives of the loss function by deriving them in different directions. Note that ReLU-like networks are continuous everywhere and piecewise C^∞ , and so is the loss, which enables us to study its directional derivatives.

The neural network is always differentiable with respect to the output weights h_{ji} . Non-differentiability only arises from input weights \mathbf{w}_i . More precisely, the network (thus the loss) is non-differentiable at \mathbf{P} if and only if a weight \mathbf{w}_i is orthogonal to some training input \mathbf{x}_k 's (see Figure 2 for an illustration). Nonetheless, when \mathbf{w}_i moves a sufficiently small distance along a fixed direction, the sign of $\mathbf{w}_i \cdot \mathbf{x}_k$ is fixed for all $k \in K$. Namely, $\mathbf{w}_i \cdot \mathbf{x}_k$ only moves on either the positive leg, the negative leg of the activation function $\rho(\cdot)$, or stays at the kink, but it will not cross the kink during the movement. With \mathbf{w}_i constrained within such a small local region, the loss is a polynomial with respect to it. This allows us to study the directional derivatives.

Definition 3.1. Consider a nonzero $\mathbf{w}_i \in \mathbb{R}^d$. The *radial direction* of \mathbf{w}_i is $\mathbf{u}_i := \frac{\mathbf{w}_i}{\|\mathbf{w}_i\|}$. Moreover, any unit vector \mathbf{v}_i orthogonal to \mathbf{u}_i is called a *tangential direction*. For $\mathbf{w}_i = \mathbf{0}$, the *radial direction* does not exist, and a *tangential direction* is defined to be any unit vector $\mathbf{v}_i \in \mathbb{R}^d$. The tangential direction is always definable given our assumption of $d > 1$.

Consider a non-zero $\mathbf{w}_i \in \mathbb{R}^d$ and let $\mathbf{w}_i' = \mathbf{w}_i + \Delta \mathbf{w}_i \neq \mathbf{w}_i$ be in the neighborhood of \mathbf{w}_i . The vector $\Delta \mathbf{w}_i$ admits a unique decomposition $\Delta \mathbf{w}_i = \Delta r_i \mathbf{u}_i + \Delta s_i \mathbf{v}_i$ with $\Delta s_i \geq 0$ and \mathbf{v}_i being a specific tangential direction of \mathbf{w}_i .

Fixing a direction for the derivative is thus equivalent to fixing a tangential direction. For a generic map f , $\frac{\partial f(\mathbf{w}_i)}{\partial r_i} := \lim_{\Delta r_i \rightarrow 0+} \frac{f(\mathbf{w}_i + \Delta r_i \mathbf{u}_i) - f(\mathbf{w}_i)}{\Delta r_i}$ and $\frac{\partial f(\mathbf{w}_i)}{\partial s_i} := \lim_{\Delta s_i \rightarrow 0+} \frac{f(\mathbf{w}_i + \Delta s_i \mathbf{v}_i) - f(\mathbf{w}_i)}{\Delta s_i}$ are termed the *radial derivative* and the *tangential derivative*.

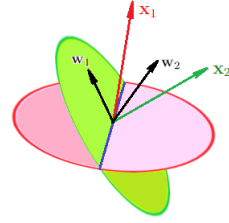


Figure 2: A diagram demonstrating the non-differentiability with respect to the input weights. Here, we show a case where input weights and training inputs are 3-dimensional. There are 2 training inputs and 2 input weights. \mathbf{w}_1 lies in a plane orthogonal to \mathbf{x}_2 . The loss is thus locally non-differentiable since it contains the term $\rho(\mathbf{w}_1 \cdot \mathbf{x}_2)$. However, we can compute the directional derivative with respect to \mathbf{w}_1 since the loss function with \mathbf{w}_1 constrained on either side of the plane or on the plane is a polynomial of \mathbf{w}_1 .

For $\mathbf{w}_i = \mathbf{0}$, we can likewise define the tangential derivative for every tangential direction \mathbf{v}_i , and by convention, set the undefinable \mathbf{u}_i and the radial derivative to zero.

To avoid any confusion, we remind the reader that the notation of $\frac{\partial}{\partial s_i}$ always implicitly implies a fixed tangential direction \mathbf{v}_i .

Lemma 3.2. *We first denote $(\hat{y}_{kj} - y_{kj}) := e_{kj}$. Then, we define the following quantities:*

$$\begin{aligned}\mathbf{d}_{ji} &:= \sum_{\substack{k: \\ \mathbf{w}_i \cdot \mathbf{x}_k > 0}} \alpha^+ e_{kj} \mathbf{x}_k + \sum_{\substack{k: \\ \mathbf{w}_i \cdot \mathbf{x}_k < 0}} \alpha^- e_{kj} \mathbf{x}_k, \\ \mathbf{d}_{ji}^{\mathbf{v}_i} &:= \sum_{\substack{k: \\ (\mathbf{w}_i + \Delta s_i \mathbf{v}_i) \cdot \mathbf{x}_k > 0}} \alpha^+ e_{kj} \mathbf{x}_k + \sum_{\substack{k: \\ (\mathbf{w}_i + \Delta s_i \mathbf{v}_i) \cdot \mathbf{x}_k < 0}} \alpha^- e_{kj} \mathbf{x}_k,\end{aligned}$$

where $\Delta s_i > 0$ is sufficiently small. We have that

$$\frac{\partial \mathcal{L}(\mathbf{P})}{\partial h_{ji}} = \mathbf{w}_i \cdot \mathbf{d}_{ji}, \quad \forall (j, i) \in J \times I, \quad (3)$$

$$\frac{\partial \mathcal{L}(\mathbf{P})}{\partial r_i} = \sum_{j \in J} h_{ji} \mathbf{d}_{ji} \cdot \mathbf{u}_i, \quad \forall i \in I, \quad (4)$$

$$\frac{\partial \mathcal{L}(\mathbf{P})}{\partial s_i} = \sum_{j \in J} h_{ji} \mathbf{d}_{ji}^{\mathbf{v}_i} \cdot \mathbf{v}_i, \quad \forall i \in I, \forall \text{ tangential direction } \mathbf{v}_i \text{'s of } \mathbf{w}_i. \quad (5)$$

The proof for the above is given in Appendix A.

It is easy to check that the network is linear with respect to the output weights and the norm of the input weights, therefore $\frac{\partial \mathcal{L}}{\partial h_{ji}}$ and $\frac{\partial \mathcal{L}}{\partial r_i}$ are continuous everywhere. But this is not the case for $\frac{\partial \mathcal{L}}{\partial s_i}$.

Note that the above formalism of directional derivative computation can be adapted for neural networks with more than one hidden layer, which will be explicated in Appendix B.

3.2 Stationary Points

Definition 3.3. A set of parameters $\bar{\mathbf{P}}$ is a stationary point of the loss in our setting if and only if the following holds: (1) $\frac{\partial \mathcal{L}(\bar{\mathbf{P}})}{\partial h_{ji}} = 0, \forall (j, i) \in J \times I$; (2) $\frac{\partial \mathcal{L}(\bar{\mathbf{P}})}{\partial r_i} = 0, \forall i \in I$; (3) $\frac{\partial \mathcal{L}(\bar{\mathbf{P}})}{\partial s_i} \geq 0, \forall i \in I, \forall$ tangential direction \mathbf{v}_i 's of $\bar{\mathbf{w}}_i$.

For differentiable functions, stationary points are defined to be where the gradient vanishes (which is included in the above definition). In our setup, we define the stationary points to be where there are no negative derivatives in the surrounding directions, which precludes any escape directions for GD. In the presence of non-differentiability, our definition admits stationary points where there exist upward slopes in one direction and the opposite, as indicated in condition 3. For directions along which the loss is continuously differentiable, we require the derivative to be 0, which explains the first two conditions. Notably, such a definition is tailored to capture the stationarity of GD by admitting positive slopes around stationary points. If we were to define stationarity for, say, gradient ascent, we would admit negative slopes around stationary points instead.

One can imagine that the stationary points defined as in Definition 3.3, no matter differentiable or not, behave similarly: GD halts in effect at these points and infinitely decelerates near them. For examples of non-differentiable local minima and saddle points, we refer the readers to Appendix C. Note that while all local minima are stationary points, this is not the case for non-differentiable local maxima. An interesting side note can be made about the rarity of local maxima on our loss landscape, whether they are differentiable or not. We can prove that a necessary condition for $\mathbf{P} \in \mathbb{R}^D$ to become a local maximum is $\hat{\mathbf{y}}_k(\mathbf{P}) = 0$ for all $k \in K$, as shown in Appendix D. Such a result extends the arguments regarding the non-existence of differentiable local maxima by [43, 44], offering a qualitative perspective of the loss landscape.

Definition 3.4. A **saddle point** is a stationary point that is not a local minimum or a local maximum.

4 Main Results

In this section, we study stationary points (Section 4.1) and find a useful sufficient condition for local minimality. We then discuss its implication for the training dynamics in vanishing initialization limit (Section 4.2) and describe how network embedding reshapes the stationary points (Section 4.3).

4.1 Properties of Stationary Points

Definition 4.1. For a stationary point, a hidden neuron i is an *escape neuron* if and only if there exist $j' \in J$ and a tangential direction \mathbf{v}_i such that $\frac{\partial \mathcal{L}(\bar{\mathbf{P}})}{\partial s_i} = \sum_{j \in J} \bar{h}_{ji} \mathbf{d}_{ji}^{\mathbf{v}_i} \cdot \mathbf{v}_i = 0$, and $\mathbf{d}_{j'i}^{\mathbf{v}_i} \cdot \mathbf{v}_i \neq 0$.

Next, we give the central argument of the present paper.

Theorem 4.2. Let $\bar{\mathbf{P}}$ be a stationary point. If $\bar{\mathbf{P}}$ does not contain escape neurons, then $\bar{\mathbf{P}}$ is a local minimum. Furthermore, this sufficient condition is also a necessary one when $|J| = 1$.

Remark 4.3. The above theorem is proved by Appendix F.1 and F.2. An intuition of Definition 4.1 and Theorem 4.2 for the scalar-output case is in Appendix E.

In the following, we refer to local minima without escape neurons as **type-1 local minima**, and refer to other local minima as **type-2 local minima**. From Theorem 4.2, all the local minima in the $|J| = 1$ case are type-1 local minima. We tend to argue that type-2 local minima should be rare and provide our reasoning in Appendix F.2.1, which will be rigorously verified in future work.

From the proof of Theorem 4.2, we can also obtain a side product: when the network output is scalar, stationary local maxima and saddle points must admit a path from them showing " 2^{nd} -order decrease", which can be formalized as below.

Corollary 4.4. Suppose $\bar{\mathbf{P}}$ is a stationary local maximum or a saddle point of \mathcal{L} with $|J| = 1$, then there exists a unit vector $\ell \in \mathbb{R}^D$ and a constant $C < 0$ such that $0 > \mathcal{L}(\bar{\mathbf{P}} + \delta \ell) - \mathcal{L}(\bar{\mathbf{P}}) \sim C\delta^2$, as $\delta \rightarrow 0+$.

Remark 4.5. This lemma will be explained in Remark F.2. It was established by characterizing the loss-decreasing path caused by the variation of escape neuron parameters. It draws similarities between the potentially non-differentiable saddle points in our setting and smooth strict saddles. It is known that saddle points in shallow linear networks are strict [45].¹ The above corollary thus serves to non-trivially extend [45] to a more complicated setting: Although ReLU networks can be understood as piecewise linear networks, stationary points in the former can reside at non-differentiable edges where the analysis for the linear networks is rendered invalid.

A Numerical Experiment for Theorem 4.2

We present a numerical experiment to illustrate Theorem 4.2. We trained a ReLU network with GD using 5 training samples (\mathbf{x}_k, y_k) . The inputs were $\mathbf{x}_k = (x_k, 1) \in \mathbb{R}^2$, and x_k 's were $-1, -0.6, -0.1, 0.3, 0.7$. The targets, y_k 's, were $0.28, -0.1, 0.03, 0.23, -0.22$. The network had 50 hidden neurons. All the parameters were initialized independently with law $\mathcal{N}(0, (5 \times 10^{-6})^2)$. The training lasted 500k epochs with a step size of 0.001. The index of the only output neuron is j_0 . Thus, the output weight associated with hidden neuron i will be denoted by $h_{j_0 i}$.

The training process is visualized in Figure 3. Figure 3a is the loss curve, where the plateaus reflect the parameters moving near stationary points. Figures 3b to 3d show the evolution of input weight orientations, input weight norms, and output weights. The input weight orientations are the counterclockwise angles between \mathbf{w}_i 's and the vector $(1, 0)$.

Each curve in Figures 3b to 3d shows the corresponding quantities associated with 1 hidden neuron. We see that most of the \mathbf{w}_i 's group at several of angles before all the parameters gain considerable amplitudes. This was well accounted for by [6, 7] for ReLU networks. We represent these hidden neurons with red and yellow in the figures and will refer to them as group 1 and group 2 neurons. One can also check that the \mathbf{w}_i 's located within $3.93 \sim 5.67 \text{ rad}$ (the grey-tinted area in Figure 3b) have $\rho(\mathbf{w}_i \cdot \mathbf{x}_k) = 0$ for all $k \in K$. Thus, according to Lemma 3.2, the gradients with respect to all

¹[45] also proved that saddle points in the *true loss* of shallow ReLU networks are strict.

the parameters associated with the related neurons are zero. These hidden neurons correspond to the black curves² in the figures and are called *dead neurons*.

We also would like to draw attention to the fact that the group 1 neurons are attracted to and stuck at a direction (≈ 2.53 rad) that is orthogonal to one of the training inputs ($\mathbf{x}_5 = (0.7, 1)$). Hence, the gradient flow encountered a non-differentiable region of the loss landscape.

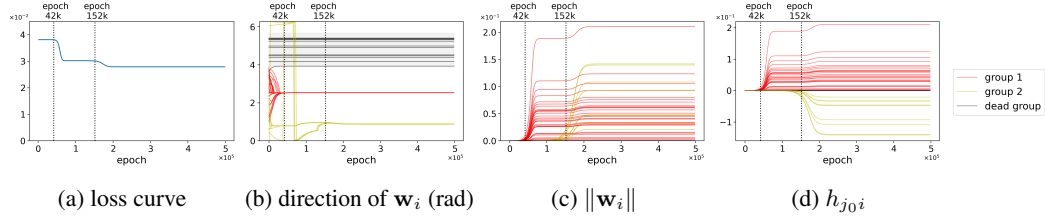


Figure 3: *Evolution of all parameters during the training process from vanishing initialization.* (a) The loss curve encounters three plateaus, the last of which corresponds to a local minimum, which we confirm with Theorem 4.2. We mark the end of the plateaus with dashed vertical lines. (b) The input weights that are not associated with dead neurons are grouped at several angles. The directions are represented with the counterclockwise angle between the \mathbf{w}_i 's and the vector $(1, 0)$. Notice that group 1 neurons are attracted to a direction orthogonal to one of the training inputs, indicating that all the stationary points involved in this training process are non-differentiable ones. (c) & (d) Grouped neurons have their amplitude increased from near-zero values, which coincides with the saddle escaping. Notice that the movements of $\|\mathbf{w}_i\|$ and $|h_{j_0 i}|$ are synchronous, as shown in Fact 4.6.

In our example, the parameters escaped from 2 saddles, which happened at about epochs $42k$ and $152k$, reflected by the rapid loss drop in Figure 3a. The last plateau in the loss curve, after the second saddle escaping, is the result of a local minimum. To numerically verify this, we perturb the parameters obtained after 500k epochs of training with small noises, and the resulting loss change is always non-negative. For details of this experiment, please refer to Appendix G.

The fact that the last plateau is a local minimum can also be confirmed by applying Theorem 4.2. In the following, we show that the stationary points that the network parameter is close to at epoch $42k$ and $152k$ have escape neurons, while the stationary point stalling the training in the end does not.

Fact 4.6 (from [4, 6]). *Throughout training, $(\|\mathbf{w}_i\|^2 - h_{j_0 i}^2)$ remains unchanged. Thus, when we initialize with a small scale, we have $\|\mathbf{w}_i\| \approx |h_{j_0 i}|$ during the entire training.*

From Definition 4.1, we know that the escape neurons for scalar-output networks have $h_{j_0 i_0} = 0$, which is also briefly explained in Appendix E. By Fact 4.6, the amplitudes of all the parameters associated with escape neurons must be small. On the other hand, dead neurons (which only exist in the ReLU case) are not escape neurons by definition.

Thus, when the network is in the vicinity of a saddle point, it must contain neurons that have small amplitudes and are not dead neurons. We will refer to such neurons as *small living neurons* in the following. They are the ones corresponding to the escape neurons in the saddle point nearby. In Figure 3, at epoch $42k$, neurons belonging to both group 1 and 2 are small living neurons; while at epoch $152k$, group 2 neurons are small living neurons. However, after the network reached the last plateau, there were no longer small living neurons, meaning the stationary point it was approaching must be a local minimum.

4.2 Saddle Escaping in the Training Dynamics

As mentioned, network training from vanishing initialization shows a *saddle-to-saddle dynamics* [4, 5, 16, 17, 32], meaning the loss experiences intermittent decreases punctuated by long plateaus. In this section, we characterize the saddle escaping process to provide a heuristic understanding of the training dynamics.

Specifically, as a direct consequence of Theorem 4.2, we have:

²Note, there are black curves in Figures 3c and 3d. They stay too close to the zero line to show up.

Consequence 4.7. *A strictly loss-decreasing path from a stationary point of the network must involve parameter variations of escape neurons.*

The above proposition is justified in Remark F.1. In the rest of this section, we apply Consequence 4.7 to understand the training dynamics of scalar-output networks from vanishing initialization. The training process can be summarized in Figure 4, which is detailed below.

At the initial phase of training, during which the parameters all have negligible amplitudes, the \mathbf{w}_i 's that are not associated with dead neurons will group at finitely many attracting directions. Such a phase of training is termed the *alignment phase*, and is described in Lemma 2 in [4], Section 4 in [5], and Lemma 4a in [6]. This can also be observed from Figure 3b. We will call the neurons whose input weights are grouped closely an *effective neuron* in the following, as they correspond to one kink position in the learned function.

After the initial alignment phase, the grouped neurons will have their amplitude increased from near-zero values. Notice that these neurons, before the amplitude increase, are small living neurons. Those that contribute to one effective neuron would have their amplitudes increased together. Such processes correspond exactly to the saddle escaping during training. This is rigorously described by Lemma 3 and 4 in [4] and Section 5 of [5] for their setup. Lemma 4b of [6] also provided non-rigorous intuitions for such process for generic cases. Thus, the amplitude increase of the small living neurons depicted by [4–6] is, in essence, exploiting a loss-decreasing path that changes the parameters of the escape neurons at the saddle point nearby.

According to Consequence 4.7, the type of saddle escaping discussed above is the only way of escaping a saddle. Other forms of saddle escaping cannot take place. This has not yet been established by previous works. Such a result stands in contrast with certain other setups. For example, in [8, 42],³ the existence of several input weights with the same direction suffices to make a strict saddle, meaning saddle escaping can take place without involving neurons with near-zero amplitude.

It is noteworthy that the amplitude increase of effective neurons from near-zero values corresponds to the emergence of one kink in the learned function. The emergence of kinks at every saddle escaping in the experiment of Figure 3 is visualized in Figure 13.

Towards Reaching Zero Loss with a Slightly Larger Initialization Scale

We have shown that the stationary point reached at the end of the numerical experiment of Section 4.1 is a local minimum, which does not yield zero loss. It turns out that if we initialize with a slightly larger standard deviation, 8.75×10^{-4} , while keeping the direction of the initialized parameters, more neuron groups will emerge, adding more expressiveness to the network, which helps to reach zero loss. The training process for this initialization scale is shown in Figure 5.

The loss curve for this initialization scheme is shown in Figure 5a, where one can observe the decrease of loss accelerated and decelerated several times. This indicates that the network parameters were also affected by several stationary points. For convenience, we marked several epochs with dotted vertical lines in Figure 5a, which is when we observe the beginnings of the accelerations in loss decrease.

The evolution of all the parameters is summarized in Figures 5b to 5d. The training process in Figure 5 differs from the one in Figure 3 in that the plateaus of the loss are less flat, meaning the trajectory of the trained parameters starting from slightly larger initialization scale did not get as

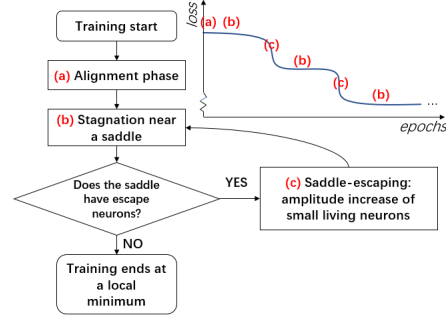


Figure 4: A flow chart for the training process. We preclude other schemes of saddle escaping, for example, by splitting aligned neurons, which is possible in [8, 42]. Also, note that saddle escaping might be accompanied by amplitude and orientation changes of other neurons, but the movements of small living neurons are indispensable.

³See Appendix K for the setting of [8]. [42] studied a teacher-student setup with true loss.

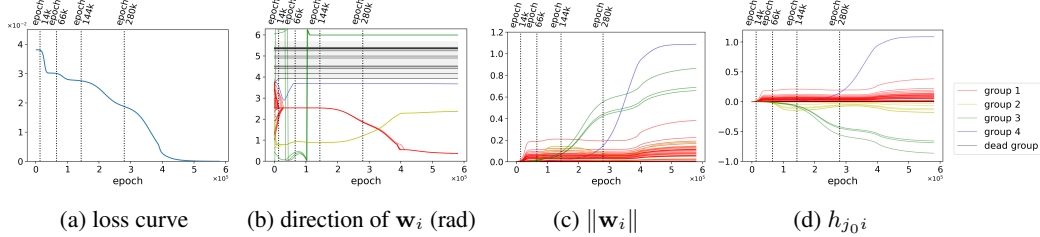


Figure 5: *Evolution of all parameters during the training process with slightly larger initialization scale.* Notice that more groups of neurons are formed compared to in Figure 3. The larger initialization scale induces a faster amplitude-increasing process, and thus a more rapid change of the attracting angles of \mathbf{w}_i 's. This avoids the merging of group 4 with group 1 and group 3 with group 2. Such merging happened in Figure 3. Additionally, note, with a slightly larger initialization scale, the trajectory of the trained parameters did not get as close to the stationary points as did the trajectory from vanishing initialization in Figure 3 [16]. Hence, the plateaus in the loss curve are no longer flat and the small living neurons no longer appear small in their norms.

close to the stationary points as did the trajectory from vanishing initialization. Such a picture was established for deep linear networks by [16] and may be carried over to our setup.

Just as in Figure 3, we color-coded the curves in Figures 5b to 5d based on the \mathbf{w}_i grouping. *We can observe that the acceleration of loss decreasing also roughly coincided with the amplitude increase of small living neurons from near-zero values, just as for the vanishing initialization.* The loss-decreasing path emanating from stationary points, which involves amplitude increasing of escape neurons, remains insightful for understanding the training dynamics in this regime. Nevertheless, in this case, the living neurons are grouped into 4 groups, corresponding to 4 kinks, which sufficed to reach zero loss. In Figure 14, we illustrate the evolution of the learned function through training. There, one can see that the network eventually fits all the data points, which is not achieved by the vanishing initialization (see Figure 13).

At a high level, the vanishing initialization limit induces a low-rank bias on the learned features [6], a phenomenon already formalized for linear networks [16]. As we increase the initialization scale, the low-rank bias is compromised for better fitting performance, indicating a tradeoff between them. Studying the minimal initialization scale that yields zero loss might be a meaningful future direction.

Towards a Full Dynamics Description

Although our result here helps us understand the start of the saddle escaping process, we are still missing a rigorous description of a complete trajectory from one saddle to another in the generic setup, which suffices to describe the entire saddle-to-saddle dynamics. [4] studied the training process with orthogonal \mathbf{x}_k 's, and [5] studied the training process where \mathbf{x}_k 's are correlated with one and only teacher feature. The former comprises two amplitude-increasing processes of two effective neurons that do not affect each other. The latter comprises only one such process. Moving forward, we still need to understand how the amplitude-increase of one effective neuron interacts with another effective neuron that already has considerable amplitudes (like what happens after epoch 152k in Figure 3).

4.3 How Network Embedding Reshapes Stationary Points

Network embedding refers to the process of instantiating a network using a wider network without changing the network function, or at least, the output of the network evaluated at all the training input \mathbf{x}_k 's. In this section, we demonstrate how network embedding reshapes stationary points, which offers a perspective on over-parameterization. In particular, we investigate the following question: Does network embedding preserve stationarity or local minimality? Such questions were partially addressed by [8] for ReLU networks. With a more complete characterization of stationary points and local minima in Sections 3.2 and 4.1, we are able to extend their results.

Following the terms defined in [8], there are three network embedding strategies for ReLU(-like) networks: unit replication, inactive units, and inactive propagation. We will showcase the usability

of our theory for unit replication, which is the most technically involving, in the main text. The full discussion for the other two embedding strategies is discussed in Appendices I and J.

The process of unit replication is illustrated in Figure 6: given a set of parameters \mathbf{P} , replace the hidden neuron $i_0 \in I$ associated with \mathbf{w}_{i_0} and h_{ji_0} , with a new set of hidden neurons $\{i_0^l; l \in L\}$ associated with weights $\mathbf{w}_{i_0^l} = \beta_l \mathbf{w}_{i_0}$ and $h_{ji_0^l} = \gamma_l h_{ji_0}$. To preserve the network function, we specify: $\beta_l > 0$, $\sum_{l \in L} \beta_l \gamma_l = 1$; $\forall l \in L, j \in J$. We can prove the following for unit replication.

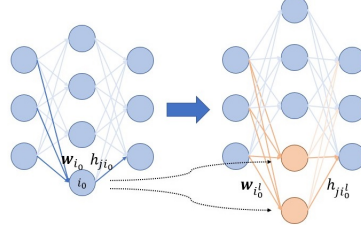


Figure 6: unit replication

Proposition 4.8. *In our setting, **unit replication** performed on neuron i_0 preserves the stationarity of a stationary point if and only if at least one of the following conditions is satisfied.*

1. *All tangential derivatives of \mathbf{w}_{i_0} are 0.*
2. *$\gamma_l \geq 0, \forall l \in L$.*

*Moreover, **unit replication** performed on neuron i_0 preserves the type-1 local minimality of a type-1 local minimum if and only if at least one of the following holds.*

1. *All tangential derivatives of \mathbf{w}_{i_0} are 0.*
2. *$\gamma_l > 0, \forall l \in L$.*

Remark 4.9. [8] was not able to discuss stationarity preservation for ReLU networks as the non-smoothness hindered the naive invocation of stationarity conditions for smooth networks. This problem has been hurdled completely in the current paper. Moreover, [8] was only able to discuss local minimality preservation for a highly restricted type of unit replication. Our proposition above nevertheless holds for all unit replication types in general, though the scope is limited to type-1 local minimality preservation.

Remark 4.10. At first sight, the statement about the preservation of type-1 local minima in the above lemma contradicts Theorem 10 of [8], which suggests that embedding a local minimum should result in a strict saddle. Nonetheless, the assumptions of that theorem does not apply to our setting. For more details, please refer to Appendix K.

It is noteworthy that unit replication always preserves stationarity for differentiable networks [32], which is no longer the case for the non-differentiable ReLU-like networks.

In addition, [46] proposed a training scheme where one neuron is split at a local minimum to create an escapable saddle point. Such a training scheme can lower the cost of training. Lemma 4.8 effectively shows how to implement such a scheme for scalar-output networks, where all the local minima are all of type-1: simply replicate a neuron whose input weight has non-zero tangential derivative and choose $\gamma_l \leq 0$. Such an insight might also be instrumental for multidimensional-output networks since type-2 local minima should be rare, as we discussed in Appendix F.2.1.

A Closing Remark

Note that the results in this section regarding stationarity preservation also serve as constructive proof that one can always embed a stationary point of a narrower network into a wider network. In other words, the stationary points of wider networks "contain" those of the narrower networks. This is termed the *network embedding principle*, discussed in [32] for smooth networks.

Moreover, this section also provides a perspective of understanding the merit of overparameterization for optimization. Stationary points and spurious local minima might worsen the performance of GD-based optimization. However, to our rescue, network embedding can cause some stationary points (local minima) to lose stationarity (local minimality). This might explain why wider networks tend to reach better training loss. It is also easy to check that embedding parameters that are not stationary points (local minima) will not result in stationary points (local minima). Similar phenomena are noted in [8, 19, 32] for smooth networks. A meaningful next step is to quantify how manifolds of saddle points and local minima scale with network width [19].

5 Summary and Discussion

In this paper, we characterize the stationarity and different types of stationary points for a one-hidden-layer network with ReLU-like activation functions. This could inspire methodologies for handling other neural network optimization landscapes that are non-differentiable. We further studied the saddle escaping process in the training dynamics with vanishing initialization and the effect of network embedding on stationary points. These can lead to several future directions. Firstly, with a better geometric understanding of the potentially non-differentiable stationary points (such as Corollary 4.4), we are better prepared to study the implicit bias of gradient flow on such landscapes that are neither smooth nor convex. Secondly, with the stationary points identified, we can study the basin of attractions of gradient flow. Thirdly, the findings of this paper might help formalize low-rank bias and generic amplitude increase processes in the future.

References

- [1] Arthur Jacot, Franck Gabriel, and Clément Hongler. Neural tangent kernel: Convergence and generalization in neural networks. *Advances in neural information processing systems*, 31, 2018.
- [2] Lenaïc Chizat, Edouard Oyallon, and Francis Bach. On lazy training in differentiable programming. *Advances in neural information processing systems*, 32, 2019.
- [3] Sanjeev Arora, Simon Du, Wei Hu, Zhiyuan Li, and Ruosong Wang. Fine-grained analysis of optimization and generalization for overparameterized two-layer neural networks. In *International Conference on Machine Learning*, pages 322–332. PMLR, 2019.
- [4] Etienne Boursier, Loucas Pillaud-Vivien, and Nicolas Flammarion. Gradient flow dynamics of shallow relu networks for square loss and orthogonal inputs. *Advances in Neural Information Processing Systems*, 35:20105–20118, 2022.
- [5] Dmitry Chistikov, Matthias Englert, and Ranko Lazic. Learning a neuron by a shallow relu network: Dynamics and implicit bias for correlated inputs, 2023.
- [6] Hartmut Maennel, Olivier Bousquet, and Sylvain Gelly. Gradient descent quantizes relu network features, 2018.
- [7] Etienne Boursier and Nicolas Flammarion. Early alignment in two-layer networks training is a two-edged sword. *arXiv preprint arXiv:2401.10791*, 2024.
- [8] Kenji Fukumizu, Shoichiro Yamaguchi, Yoh-ichi Mototake, and Mirai Tanaka. Semi-flat minima and saddle points by embedding neural networks to overparameterization. In H. Wallach, H. Larochelle, A. Beygelzimer, F. d’Alché-Buc, E. Fox, and R. Garnett, editors, *Advances in Neural Information Processing Systems*, volume 32. Curran Associates, Inc., 2019. URL https://proceedings.neurips.cc/paper_files/paper/2019/file/a4ee59dd868ba016ed2de90d330acb6a-Paper.pdf.
- [9] Fengxiang He, Bohan Wang, and Dacheng Tao. Piecewise linear activations substantially shape the loss surfaces of neural networks. In *International Conference on Learning Representations*, 2020. URL <https://openreview.net/forum?id=B1x6BTEKwr>.
- [10] Arsalan Sharifnassab, Saber Salehkaleybar, and S. Jamaloddin Golestani. Bounds on overparameterization for guaranteed existence of descent paths in shallow relu networks. In *International Conference on Learning Representations*, 2020.
- [11] Bo Liu, Zhaoying Liu, Ting Zhang, and Tongtong Yuan. Non-differentiable saddle points and sub-optimal local minima exist for deep relu networks. *Neural Networks*, 144:75–89, 2021. ISSN 0893-6080. doi: <https://doi.org/10.1016/j.neunet.2021.08.005>. URL <https://www.sciencedirect.com/science/article/pii/S0893608021003105>.
- [12] Yossi Arjevani and Michael Field. Analytic study of families of spurious minima in two-layer relu neural networks: A tale of symmetry ii, 2021.

- [13] Berfin Şimşek, Amire Bendjeddou, Wulfram Gerstner, and Johanni Brea. Should under-parameterized student networks copy or average teacher weights? *arXiv preprint arXiv:2311.01644*, 2023.
- [14] David Saad and Sara A Solla. On-line learning in soft committee machines. *Physical Review E*, 52(4):4225, 1995.
- [15] Shun-ichi Amari. Natural Gradient Works Efficiently in Learning. *Neural Computation*, 10(2):251–276, 02 1998. ISSN 0899-7667. doi: 10.1162/089976698300017746. URL <https://doi.org/10.1162/089976698300017746>.
- [16] Arthur Jacot, François Ged, Berfin Şimşek, Clément Hongler, and Franck Gabriel. Saddle-to-saddle dynamics in deep linear networks: Small initialization training, symmetry, and sparsity, 2022.
- [17] Scott Pesme and Nicolas Flammarion. Saddle-to-saddle dynamics in diagonal linear networks. *Advances in Neural Information Processing Systems*, 36, 2024.
- [18] K. Fukumizu and S. Amari. Local minima and plateaus in hierarchical structures of multilayer perceptrons. *Neural Networks*, 13(3):317–327, 2000. ISSN 0893-6080. doi: [https://doi.org/10.1016/S0893-6080\(00\)00009-5](https://doi.org/10.1016/S0893-6080(00)00009-5). URL <https://www.sciencedirect.com/science/article/pii/S0893608000000095>.
- [19] Berfin Şimşek, François Ged, Arthur Jacot, Francesco Spadaro, Clement Hongler, Wulfram Gerstner, and Johanni Brea. Geometry of the loss landscape in overparameterized neural networks: Symmetries and invariances. In Marina Meila and Tong Zhang, editors, *Proceedings of the 38th International Conference on Machine Learning*, volume 139 of *Proceedings of Machine Learning Research*, pages 9722–9732. PMLR, 18–24 Jul 2021. URL <https://proceedings.mlr.press/v139/simsek21a.html>.
- [20] El Mehdi Achour, François Malgouyres, and Sébastien Gerchinovitz. The loss landscape of deep linear neural networks: a second-order analysis, 2022.
- [21] Jason D. Lee, Ioannis Panageas, Georgios Piliouras, Max Simchowitz, Michael I. Jordan, and Benjamin Recht. First-order methods almost always avoid saddle points, 2017.
- [22] Jason D. Lee, Max Simchowitz, Michael I. Jordan, and Benjamin Recht. Gradient descent converges to minimizers, 2016.
- [23] El Mehdi Achour, François Malgouyres, and Sébastien Gerchinovitz. Global minimizers, strict and non-strict saddle points, and implicit regularization for deep linear neural networks. 2021.
- [24] Chi Jin, Rong Ge, Praneeth Netrapalli, Sham M. Kakade, and Michael I. Jordan. How to escape saddle points efficiently. *CoRR*, abs/1703.00887, 2017. URL <http://arxiv.org/abs/1703.00887>.
- [25] Hadi Daneshmand, Jonas Moritz Kohler, Aurélien Lucchi, and Thomas Hofmann. Escaping saddles with stochastic gradients. *CoRR*, abs/1803.05999, 2018. URL <http://arxiv.org/abs/1803.05999>.
- [26] Liu Ziyin, Botao Li, James B. Simon, and Masahito Ueda. Sgd with a constant large learning rate can converge to local maxima, 2023.
- [27] Yi Zhou and Yingbin Liang. Critical points of linear neural networks: Analytical forms and landscape properties. In *International Conference on Learning Representations*, 2018. URL <https://openreview.net/forum?id=SysEexbRb>.
- [28] Justin Sahs, Ryan Pyle, Aneel Damaraju, Josue Ortega Caro, Onur Tavaslioglu, Andy Lu, Fabio Anselmi, and Ankit B. Patel. Shallow univariate relu networks as splines: Initialization, loss surface, hessian, and gradient flow dynamics. *Frontiers in Artificial Intelligence*, 5, 2022. ISSN 2624-8212. doi: 10.3389/frai.2022.889981. URL <https://www.frontiersin.org/articles/10.3389/frai.2022.889981>.

- [29] Patrick Cheridito, Arnulf Jentzen, and Florian Rossmannek. Landscape analysis for shallow neural networks: Complete classification of critical points for affine target functions. *Journal of Nonlinear Science*, 32(5), jul 2022. doi: 10.1007/s00332-022-09823-8. URL <https://doi.org/10.1007/s00332-022-09823-8>.
- [30] Zeyuan Allen-Zhu, Yuanzhi Li, and Yingyu Liang. Learning and generalization in overparameterized neural networks, going beyond two layers. *Advances in neural information processing systems*, 32, 2019.
- [31] Greg Yang and J. Edward Hu. Feature learning in infinite-width neural networks. *CoRR*, abs/2011.14522, 2020. URL <https://arxiv.org/abs/2011.14522>.
- [32] Yaoyu Zhang, Zhongwang Zhang, Tao Luo, and Zhiqin J Xu. Embedding principle of loss landscape of deep neural networks. *Advances in Neural Information Processing Systems*, 34: 14848–14859, 2021.
- [33] Tao Luo, Zhi-Qin John Xu, Zheng Ma, and Yaoyu Zhang. Phase diagram for two-layer relu neural networks at infinite-width limit. *The Journal of Machine Learning Research*, 22(1): 3327–3373, 2021.
- [34] Roi Livni, Shai Shalev-Shwartz, and Ohad Shamir. On the computational efficiency of training neural networks. *Advances in neural information processing systems*, 27, 2014.
- [35] Itay Safran and Ohad Shamir. On the quality of the initial basin in overspecified neural networks. In *International Conference on Machine Learning*, 2015.
- [36] Daniel Soudry and Yair Carmon. No bad local minima: Data independent training error guarantees for multilayer neural networks. *ArXiv*, abs/1605.08361, 2016.
- [37] Quynh Nguyen and Matthias Hein. The loss surface of deep and wide neural networks. *CoRR*, abs/1704.08045, 2017. URL <http://arxiv.org/abs/1704.08045>.
- [38] Daniel Soudry and Elad Hoffer. Exponentially vanishing sub-optimal local minima in multilayer neural networks, 2017.
- [39] Simon Du and Jason Lee. On the power of over-parametrization in neural networks with quadratic activation. In Jennifer Dy and Andreas Krause, editors, *Proceedings of the 35th International Conference on Machine Learning*, volume 80 of *Proceedings of Machine Learning Research*, pages 1329–1338. PMLR, 10–15 Jul 2018. URL <https://proceedings.mlr.press/v80/du18a.html>.
- [40] Luca Venturi, Afonso S. Bandeira, and Joan Bruna. Spurious valleys in one-hidden-layer neural network optimization landscapes. *Journal of Machine Learning Research*, 20(133):1–34, 2019. URL <http://jmlr.org/papers/v20/18-674.html>.
- [41] Mahdi Soltanolkotabi, Adel Javanmard, and Jason D. Lee. Theoretical insights into the optimization landscape of over-parameterized shallow neural networks, 2022.
- [42] Itay Safran, Gilad Yehudai, and Ohad Shamir. The effects of mild over-parameterization on the optimization landscape of shallow relu neural networks. In *Annual Conference on Learning Theory*, 2020. URL <https://api.semanticscholar.org/CorpusID:219176870>.
- [43] Bo Liu. Understanding the loss landscape of one-hidden-layer relu networks. *Knowledge-Based Systems*, 220:106923, 2021. ISSN 0950-7051. doi: <https://doi.org/10.1016/j.knosys.2021.106923>. URL <https://www.sciencedirect.com/science/article/pii/S0950705121001866>.
- [44] Aleksandar Botev, Hippolyt Ritter, and David Barber. Practical gauss-newton optimisation for deep learning. In *International Conference on Machine Learning*, pages 557–565. PMLR, 2017.
- [45] Kenji Kawaguchi. Deep learning without poor local minima. In D. Lee, M. Sugiyama, U. Luxburg, I. Guyon, and R. Garnett, editors, *Advances in Neural Information Processing Systems*, volume 29. Curran Associates, Inc., 2016. URL https://proceedings.neurips.cc/paper_files/paper/2016/file/f2fc990265c712c49d51a18a32b39f0c-Paper.pdf.

- [46] Lemeng Wu, Dilin Wang, and Qiang Liu. Splitting steepest descent for growing neural architectures. In H. Wallach, H. Larochelle, A. Beygelzimer, F. d'Alché-Buc, E. Fox, and R. Garnett, editors, *Advances in Neural Information Processing Systems*, volume 32. Curran Associates, Inc., 2019. URL https://proceedings.neurips.cc/paper_files/paper/2019/file/3a01fc0853ebeba94fde4d1cc6fb842a-Paper.pdf.

A Proof of Lemma 3.2

A.1 Derivation of Equation (3)

We compute

$$\frac{\partial \hat{y}_{kj'}}{\partial h_{ji}} = \frac{\partial}{\partial h_{ji}} \sum_{i' \in I} h_{ji'} \rho(\mathbf{w}_{i'} \cdot \mathbf{x}_k) = \mathbb{1}_{\{j=j'\}} \rho(\mathbf{w}_i \cdot \mathbf{x}_k).$$

Thus, we have

$$\frac{\partial}{\partial h_{ji}} \mathcal{L}(\mathbf{P}) = \frac{\partial}{\partial h_{ji}} \left(\frac{1}{2} \sum_{j' \in J} \sum_{k \in K} (\hat{y}_{kj'} - y_{kj'})^2 \right) = \sum_{j' \in J} \sum_{k \in K} e_{kj'} \frac{\partial \hat{y}_{kj'}}{\partial h_{ji}} = \sum_{k \in K} e_{kj} \rho(\mathbf{w}_i \cdot \mathbf{x}_k) = \mathbf{w}_i \cdot \mathbf{d}_{ji},$$

A.2 Derivation of Equation (4)

For all $x, y \in \mathbb{R}$, define

$$\tilde{\rho}_y(x) := \begin{cases} \alpha_+ x & \text{if } y > 0, \\ \rho(x) & \text{if } y = 0, \\ \alpha_- x & \text{if } y < 0. \end{cases}$$

The map $\tilde{\rho}(\cdot)$ will be convenient to compute the following derivatives.

Let i be such that $\|\mathbf{w}_i\| \neq 0$, let $\mathbf{u}_i = \frac{\mathbf{w}_i}{\|\mathbf{w}_i\|}$. Recall that the derivatives $\frac{\partial}{\partial r_i}, \frac{\partial}{\partial s_i}$ are defined below Definition 3.1. Below, we write $\mathbf{w}_i = r_i \mathbf{u}_i$ and take the derivative at $r_i = \|\mathbf{w}_i\|$. Note that $\rho(r_i \mathbf{w}_i \cdot \mathbf{x}_k) = r_i \rho(\mathbf{w}_i \cdot \mathbf{x}_k)$, that is, along the direction \mathbf{u}_i , the activation ρ is linear. We thus have that

$$\frac{\partial \hat{y}_{kj}}{\partial r_i} = h_{ji} \frac{\partial \rho(r_i \mathbf{u}_i \cdot \mathbf{x}_k)}{\partial r_i} = h_{ji} \rho(\mathbf{u}_i \cdot \mathbf{x}_k).$$

We then get

$$\begin{aligned} \frac{\partial \mathcal{L}(\mathbf{P})}{\partial r_i} &= \sum_{j \in J} \sum_{k \in K} e_{kj} \frac{\partial \hat{y}_{kj}}{\partial r_i} = \sum_{j \in J} \sum_{k \in K} e_{kj} h_{ji} \rho(\mathbf{u}_i \cdot \mathbf{x}_k) \\ &= \sum_{j \in J} \sum_{k \in K} e_{kj} h_{ji} \mathbf{u}_i \cdot \tilde{\rho}_{\mathbf{u}_i \cdot \mathbf{x}_k}(\mathbf{x}_k) \\ &= \sum_{j \in J} h_{ji} \mathbf{u}_i \cdot \left(\sum_{\substack{k: \\ \mathbf{w}_i \cdot \mathbf{x}_k > 0}} \alpha^+ e_{kj} \mathbf{x}_k + \sum_{\substack{k: \\ \mathbf{w}_i \cdot \mathbf{x}_k < 0}} \alpha^- e_{kj} \mathbf{x}_k \right) \\ &= \sum_{j \in J} h_{ji} \mathbf{u}_i \cdot \mathbf{d}_{ji}, \end{aligned}$$

where \mathbf{d}_{ji} was defined in Lemma 3.2.

A.3 Derivation of Equation (5)

Recall that when taking the derivative $\frac{\partial}{\partial s_i}$, a specific direction \mathbf{v}_i is chosen. One can check that

$$\begin{aligned} \frac{\partial \rho(\mathbf{w}_i \cdot \mathbf{x}_k)}{\partial s_i} &= \mathbb{1}_{\{\mathbf{w}_i \cdot \mathbf{x}_k \neq 0\}} \tilde{\rho}_{\mathbf{w}_i \cdot \mathbf{x}_k}(\mathbf{v}_i \cdot \mathbf{x}_k) + \mathbb{1}_{\{\mathbf{w}_i \cdot \mathbf{x}_k = 0\}} \rho(\mathbf{v}_i \cdot \mathbf{x}_k) \\ &= \tilde{\rho}_{\mathbf{w}_i \cdot \mathbf{x}_k}(\mathbf{v}_i \cdot \mathbf{x}_k) \end{aligned}$$

We thus obtain:

$$\frac{\partial \hat{y}_{kj}}{\partial s_i} = h_{ji} \frac{\partial \rho(\mathbf{w}_i \cdot \mathbf{x}_k)}{\partial s_i} = h_{ji} \tilde{\rho}_{\mathbf{w}_i \cdot \mathbf{x}_k}(\mathbf{v}_i \cdot \mathbf{x}_k)$$

We thus have that

$$\begin{aligned}
\frac{\partial \mathcal{L}(\mathbf{P})}{\partial s_i} &= \sum_{j \in J} \sum_{k \in K} e_{kj} \frac{\partial \hat{y}_{kj}(\mathbf{P})}{\partial s_i} = \sum_{j \in J} \sum_{k \in K} e_{kj} \tilde{\rho}_{\mathbf{w}_i \cdot \mathbf{x}_k}(\mathbf{v}_i \cdot \mathbf{x}_k) \\
&= \sum_{j \in J} \sum_{k \in K} e_{kj} \mathbf{v}_i \cdot (\mathbb{1}_{\{\mathbf{w}_i \cdot \mathbf{x}_k \neq 0\}} \tilde{\rho}_{\mathbf{w}_i \cdot \mathbf{x}_k}(\mathbf{x}_k) + \mathbb{1}_{\{\mathbf{w}_i \cdot \mathbf{x}_k = 0\}} \tilde{\rho}_{\mathbf{v}_i \cdot \mathbf{x}_k}(\mathbf{x}_k)) \\
&= \sum_{\substack{k: \\ (\mathbf{w}_i + \Delta s_i \mathbf{v}_i) \cdot \mathbf{x}_k > 0}} \alpha^+ e_{kj} \mathbf{x}_k + \sum_{\substack{k: \\ (\mathbf{w}_i + \Delta s_i \mathbf{v}_i) \cdot \mathbf{x}_k < 0}} \alpha^- e_{kj} \mathbf{x}_k \\
&= \sum_{j \in J} h_{ji} \mathbf{v}_i \cdot \mathbf{d}_{ji}^{\mathbf{v}_i},
\end{aligned}$$

where $\Delta s_i > 0$ is sufficiently small and where $\mathbf{d}_{ji}^{\mathbf{v}_i}$ was defined in Lemma 3.2.

B Extending Lemma 3.2 to Networks with Multiple Hidden Layers

In this section, we demonstrate how we can compute the radial and tangential derivatives with respect to weights that are in ReLU-like networks with multiple hidden layers.

The notation of this section inherits from the one-hidden-layer case for the most part. Nonetheless, we augment the notation for the hidden layer weights with an index to number the layers.

The training inputs are \mathbf{x}_k 's, and we also denote them by $\mathbf{x}_k^{(0)} \in \mathbb{R}^{|I_0|}$ (for the sake of notation simplicity). The training targets are $\mathbf{y}_k \in \mathbb{R}^{|J|}$. The input weight matrix in hidden layer $l \in \{1, \dots, L\}$ is $W^{(l)} \in \mathbb{R}^{|I_{l-1}| \times |I_l|}$. I_l is the set of hidden neurons in layer l . The hidden neuron weights corresponding to one row of $W^{(l)}$ is $\mathbf{w}_i^{(l)}$, where $i \in I_l$. The output weight matrix is $H \in \mathbb{R}^{|J| \times |I_L|}$, each row of which is \mathbf{h}_j with $j \in J$.

The neural network is defined recursively with the following:

$$\eta_k^{(l)} = W^{(l)} \mathbf{x}_k^{(l-1)}, \quad \mathbf{x}_k^{(l)} = \rho(\eta_k^{(l)}), \quad \forall l \in \{1, 2, \dots, L\}; \quad \hat{\mathbf{y}}_k = H \mathbf{x}_k^{(L)}.$$

B.1 Output Weight Derivatives

We first compute the network outputs' derivatives with respect to the output weights.

$$\frac{\partial \hat{y}_{kj'}}{\partial \mathbf{h}_j} = \mathbb{1}_{j=j'} \mathbf{x}_k^{(L)}$$

Then we have:

$$\frac{\partial \mathcal{L}}{\partial \mathbf{h}_j} = \sum_{k \in K} \sum_{j' \in J} e_{kj'} \frac{\partial y_{kj'}}{\partial \mathbf{h}_j} = \sum_{k \in K} e_{kj} \mathbf{x}_k^{(L)}$$

B.2 Hidden Neuron Weight Derivatives

For a specific layer $l^0 \in \{1, 2, \dots, L\}$, and a specific direction of $\Delta \mathbf{w}_i^{(l^0)} = \Delta r_i^{(l^0)} \mathbf{u}_i^{(l^0)} + \Delta s_i^{(l^0)} \mathbf{v}_i^{(l^0)}$, where $\mathbf{u}_i^{(l^0)}$ and $\mathbf{v}_i^{(l^0)}$ are the radial direction and a tangential direction of $\mathbf{w}_i^{(l^0)}$, and $i \in I_{l^0}$, we compute the radial derivative and tangential derivative.

Radial Derivative

$$\frac{\partial \hat{y}_{kj}}{\partial r_i^{(l^0)}} = \frac{\partial \hat{y}_{kj}}{\partial x_{ki}^{(l^0)}} \frac{\partial x_{ki}^{(l^0)}}{\partial r_i^{(l^0)}} = \frac{\partial \hat{y}_{kj}}{\partial x_{ki}^{(l^0)}} \rho(\mathbf{u}_i^{(l^0)} \cdot \mathbf{x}_k^{(l^0-1)})$$

Thus:

$$\begin{aligned}\frac{\partial \mathcal{L}}{\partial r_i^{(l^0)}} &= \sum_{j \in J} \sum_{k \in K} e_{kj} \frac{\partial \hat{y}_{kj}}{\partial r_i^{(l^0)}} \\ &= \sum_{j \in J} \sum_{k \in K} e_{kj} \frac{\partial \hat{y}_{kj}}{\partial x_{ki}^{(l^0)}} \rho(\mathbf{u}_i^{(l^0)} \cdot \mathbf{x}_k^{(l^0-1)}),\end{aligned}$$

which is reminiscent of the one-hidden-layer case.

Tangential Derivative

Again, we start by computing the output's derivative.

$$\frac{\partial \hat{y}_{kj}}{\partial s_i^{(l^0)}} = \frac{\partial \hat{y}_{kj}}{\partial x_{ki}^{(l^0)}} \frac{\partial x_{ki}^{(l^0)}}{\partial s_i^{(l^0)}} = \frac{\partial \hat{y}_{kj}}{\partial x_{ki}^{(l^0)}} \tilde{\rho}_{\mathbf{w}_i^{(l^0)} \cdot \mathbf{x}_k^{(l^0-1)}}(\mathbf{v}_i^{(l^0)} \cdot \mathbf{x}_k^{(l^0-1)})$$

Thus:

$$\begin{aligned}\frac{\partial \mathcal{L}}{\partial s_i^{(l^0)}} &= \sum_{j \in J} \sum_{k \in K} e_{kj} \frac{\partial \hat{y}_{kj}}{\partial s_i^{(l^0)}} \\ &= \sum_{j \in J} \sum_{k \in K} e_{kj} \frac{\partial \hat{y}_{kj}}{\partial x_{ki}^{(l^0)}} \tilde{\rho}_{\mathbf{w}_i^{(l^0)} \cdot \mathbf{x}_k^{(l^0-1)}}(\mathbf{v}_i^{(l^0)} \cdot \mathbf{x}_k^{(l^0-1)}) \\ &= \sum_{j \in J} \sum_{k: (\mathbf{w}_i^{(l^0)} + \Delta s_i \mathbf{v}_i) \cdot \mathbf{x}_k > 0} \alpha^+ e_{kj} \frac{\partial \hat{y}_{kj}}{\partial x_{ki}^{(l^0)}} \mathbf{v}_i^{(l^0)} \cdot \mathbf{x}_k^{(l^0-1)} \\ &\quad + \sum_{j \in J} \sum_{k: (\mathbf{w}_i^{(l^0)} + \Delta s_i \mathbf{v}_i) \cdot \mathbf{x}_k < 0} \alpha^- e_{kj} \frac{\partial \hat{y}_{kj}}{\partial x_{ki}^{(l^0)}} \mathbf{v}_i^{(l^0)} \cdot \mathbf{x}_k^{(l^0-1)},\end{aligned}$$

where $\Delta s_i > 0$ is arbitrarily small. Again, this is reminiscent of the one-hidden-layer case.

Computing $\frac{\partial \hat{y}_{kj}}{\partial x_{ki}^{(l^0)}}$

$\frac{\partial \hat{y}_{kj}}{\partial x_{ki}^{(l^0)}}$ shows up in the formula of radial directional derivative and tangential directional derivative. In this part, we compute the vector containing this value, $\frac{\partial \hat{y}_{kj}}{\partial \mathbf{x}_k^{(l^0)}}$. This derivative can be derived from the routine of back-propagation, adapted to accommodate the non-smoothness of the activation function.

We first compute:

$$\frac{\partial \hat{\mathbf{y}}_k}{\partial \mathbf{x}_k^{(L)}} = H^\top$$

Then, for $l \in \{l^0, l^0 + 1, \dots, L - 1\}$, we have:

$$\begin{aligned}\frac{\partial \hat{\mathbf{y}}_k}{\partial \mathbf{x}_k^{(l)}} &= \frac{\partial \boldsymbol{\eta}_k^{(l+1)}}{\partial \mathbf{x}_k^{(l)}} \frac{\partial \mathbf{x}_k^{(l+1)}}{\partial \boldsymbol{\eta}_k^{(l+1)}} \frac{\partial \hat{\mathbf{y}}_k}{\partial \mathbf{x}_k^{(l+1)}} \\ &= \left(W_l^{(l)}\right)^\top \text{diag}(\boldsymbol{\alpha}_k^{(l)}) \frac{\partial \hat{\mathbf{y}}_k}{\partial \mathbf{x}_k^{(l+1)}},\end{aligned}$$

where the vector of $\boldsymbol{\alpha}_k^{(l)}$ may be componentwise defined as:

$$\alpha_{ki}^{(l)} = \begin{cases} \alpha^+ & \text{if } \eta_{ki}^{(l)} + \Delta \eta_{ki}^{(l)} (\Delta \mathbf{w}_i^{(l^0)}) > 0 \\ 0 & \text{if } \eta_{ki}^{(l)} + \Delta \eta_{ki}^{(l)} (\Delta \mathbf{w}_i^{(l^0)}) = 0 \\ \alpha^- & \text{if } \eta_{ki}^{(l)} + \Delta \eta_{ki}^{(l)} (\Delta \mathbf{w}_i^{(l^0)}) < 0 \end{cases}$$

Here, $\Delta\eta_{ki}^{(l)}$ ($\Delta\mathbf{w}_i^{(l^0)}$) is the change of $\eta_{ki}^{(l)}$ when an arbitrarily small perturbation of $\Delta\mathbf{w}_i^{(l^0)}$ is applied to $\mathbf{w}_i^{(l^0)}$. When computing radial derivative, such perturbation can be taken as $\Delta\mathbf{w}_i^{(l^0)} = \Delta r_i^{(l^0)} \mathbf{u}_i^{(l^0)}$. When computing the tangential derivative, such perturbation can be taken as $\Delta\mathbf{w}_i^{(l^0)} = \Delta s_i^{(l^0)} \mathbf{v}_i^{(l^0)}$.

C Examples of Non-differentiable Stationary Points

Here, we give two examples of non-differentiable stationary points under GD. We remind the readers that, in the presence of non-differentiability, stationarity is defined as the absence of directions with negative first-order directional derivatives.

C.1 A Non-differentiable Local Minimum

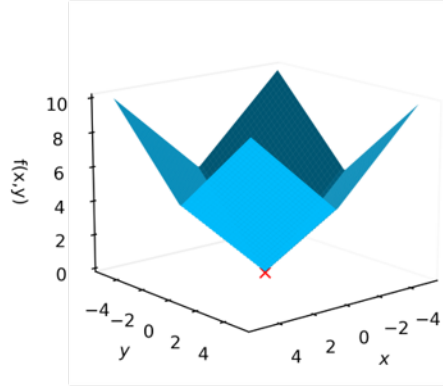


Figure 7: A non-differentiable local minimum

In Figure 7, we show a non-differentiable local minimum of the function $f(x, y) = |x + y|$, which is the origin and denoted by the red x. It is not hard to see that GD performed on the function will approach this point and stop there (or bounce in its vicinity, which can be taken as "GD halts in effect", as phrased in Section 3.2).

C.2 A Non-differentiable Saddle Point

In Figure 8a, we illustrate a non-differentiable saddle point and GD's behavior near it. The function we investigate in this example is the following:

$$f(x, y) = \begin{cases} y^2 + x & \text{if } x > 0 \text{ and } y > 0 \\ -y^2 + x & \text{if } x > 0 \text{ and } y \leq 0 \\ y^2 - x & \text{if } x \leq 0 \text{ and } y > 0 \\ -y^2 - x & \text{if } x \leq 0 \text{ and } y \leq 0 \end{cases}, \quad (6)$$

which is showed in Figure 8a. The origin is a non-differentiable saddle point. If we perform GD starting from $(x, y) = (1e^{-6}, 1)$, the trajectory of GD will be as shown in Figure 8b, and the change of function value during the GD process will be as shown in Figure 8c. The behavior of GD is much like that near a differentiable saddle. However, one can show that, in this case, given a step size smaller than $\frac{1}{4}$, the non-differentiable saddle point is non-escapable by GD, even though it has second-order decreasing directions. This is in contrast with strict differentiable saddles, which are almost always escapable by GD [21, 22, 24, 25].

D Rarity of Local Maxima

In theory, local maxima can exist in our setting [27]. Nonetheless, the theorem below suggests that they are extremely rare.

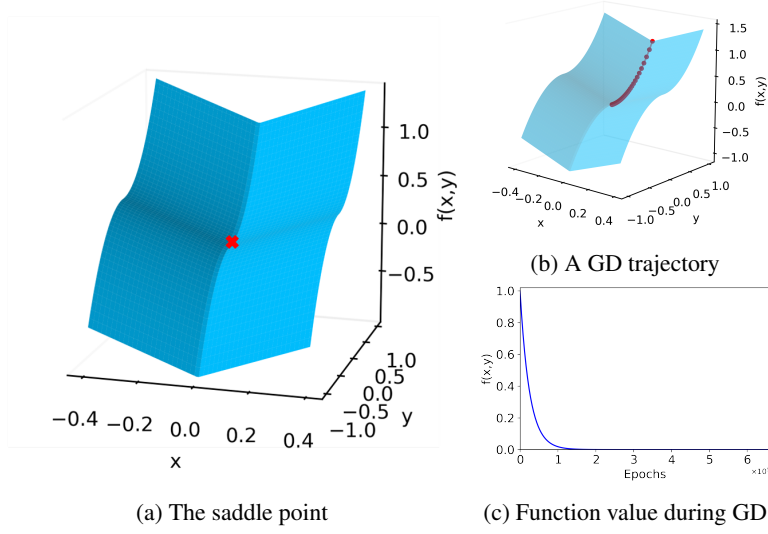


Figure 8: A non-differentiable saddle point

Theorem D.1. *If there exists some input weight vector \mathbf{w}_i in $\mathbf{P} \in \mathbb{R}^D$ satisfying $\rho(\mathbf{w}_i \cdot \mathbf{x}_k) \neq 0$ for some input \mathbf{x}_k , then, \mathbf{P} cannot be a local maximum.*

Proof. We need to show that when the parameters \mathbf{P} satisfies the sufficient condition in Theorem D.1, there exist perturbations leading to strict loss increase. Let us focus on one of the hidden neurons (with the subscript of i) that has $\rho(\mathbf{w}_i \cdot \mathbf{x}_k) \neq 0$ for some $k \in K$. Let us also specify an output neuron indexed with j . We will construct a strictly loss-increasing path only by modifying h_{ji} .

Here we could simply use the derivatives that we computed before and show it's positive:

$$\begin{aligned} \frac{\partial \mathcal{L}(\bar{\mathbf{P}})}{\partial h_{ji}} &= \sum_{k \in K} e_{kj} \rho(\mathbf{w}_i \cdot \mathbf{x}_k), \\ \frac{\partial^2 \mathcal{L}(\bar{\mathbf{P}})}{\partial h_{ji}^2} &= \sum_{k \in K} \rho(\mathbf{w}_i \cdot \mathbf{x}_k)^2. \end{aligned}$$

Hence, we see that either the first derivative is non-zero, in which case there is a loss-increasing direction since the loss is continuously differentiable in h_{ji} , or the first derivative is null and the second derivative is strictly positive, in which case we also get a loss-increasing path.

□

Remark D.2. [43] proved the absence of differentiable local maxima for $\|J\| = 1$, and [44] precluded the existence of differentiable strict local maxima for networks with piecewise linear activation functions. Here, we provide a more generic conclusion, that if \mathbf{P} is a local maximum, no matter whether differentiable or not, then all input weight vectors are not "activating" any of the inputs in the dataset, meaning $\hat{y}_k(\mathbf{P}) = 0$ for all $k \in K$.

E Intuition of Definition 4.1 and Theorem 4.2

When the output dimension is one, we can understand why the escape neurons, as defined, can lead to loss-decreasing path. Let us denote the only output neuron with the subscript of j_0 . For the escape neuron, we have that for some tangential direction \mathbf{v}_i fixed, $\frac{\partial \mathcal{L}(\bar{\mathbf{P}})}{\partial s_i} = \bar{h}_{j_0 i} \mathbf{d}_{j_0 i}^{\mathbf{v}_i} \cdot \mathbf{v}_i = 0$ and $\mathbf{d}_{j_0 i}^{\mathbf{v}_i} \cdot \mathbf{v}_i \neq 0$. This must mean that $\bar{h}_{j_0 i} = 0$. If we slightly perturb $\bar{h}_{j_0 i}$ such that it has a different sign than $\mathbf{d}_{j_0 i}^{\mathbf{v}_i} \cdot \mathbf{v}_i$, then the tangential derivative $\frac{\partial \mathcal{L}(\bar{\mathbf{P}})}{\partial s_i}$ after the perturbation is negative, indicating a loss-decreasing direction.

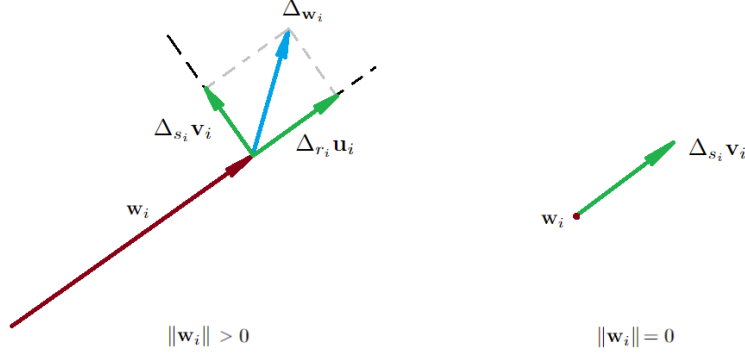


Figure 9: Breakdown of perturbation applied on input weights. Left: Perturbation on \mathbf{w}_i with $\|\mathbf{w}_i\| > 0$ can be decomposed into the radial direction \mathbf{u}_i and the tangential direction \mathbf{v}_i . Right: Perturbation applied on a zero input weight can only be decomposed into one direction \mathbf{v}_i .

F Proof of Theorem 4.2

For brevity, we use $(a_l)_{l \in L}$ to denote a vector that is composed by stacking together the a_l 's with $l \in L$.

F.1 Proof of the Sufficiency

We start by introducing the directional derivatives of the loss. Fix a unit vector $\Delta \in \mathbb{R}^D$ in the parameter space, along which we investigate the derivative. By doing so, we also fix the vectors $\mathbf{u}_i, \mathbf{v}_i$ for all $i \in I$, since the decomposition $\Delta_{\mathbf{w}_i} = \Delta_{r_i} \mathbf{u}_i + \Delta_{s_i} \mathbf{v}_i$ is unique, i.e. there exists a unique unit tangential vector \mathbf{v}_i orthogonal with $\mathbf{u}_i = \frac{\mathbf{w}_i}{\|\mathbf{w}_i\|}$ and unique $r_i, s_i \geq 0$. By convention, if $\mathbf{w}_i = 0$, we set $\mathbf{u}_i = 0$ and $r_i = 0$. See Figure 9 for a visualization of $\mathbf{u}_i, \mathbf{v}_i$.

The directional derivative of the loss in direction Δ is then defined by

$$\partial_{\Delta} \mathcal{L}(\mathbf{P}) := \lim_{\epsilon \rightarrow 0+} \frac{\mathcal{L}(\mathbf{P} + \epsilon \Delta) - \mathcal{L}(\mathbf{P})}{\epsilon}.$$

Note that the limit always exists, since, as we saw in previous sections, the partial derivatives $\frac{\partial \mathcal{L}(\mathbf{P})}{\partial s_i}, \frac{\partial \mathcal{L}(\mathbf{P})}{\partial r_i}$ are always well defined. However, we stress that because of the non-differentiability, we can have that $\partial_{\Delta} \mathcal{L}(\mathbf{P}) \neq -\partial_{-\Delta} \mathcal{L}(\mathbf{P})$.

Consider a stationary point $\bar{\mathbf{P}}$ of \mathcal{L} with no escape neuron. Also, consider a direction Δ such that $\partial_{\Delta} \mathcal{L}(\bar{\mathbf{P}}) = 0$. *Directions with $\partial_{\Delta} \mathcal{L}(\bar{\mathbf{P}}) > 0$ (which is possible due to the positive tangential slope at input weights) are guaranteed to increase the loss locally.* Our strategy is to show that the directional derivatives of higher orders are non-negative. For example, at order 2 this means that

$$\partial_{\Delta}^2 \mathcal{L}(\bar{\mathbf{P}}) := \lim_{\epsilon \rightarrow 0+} \frac{\partial_{\Delta} \mathcal{L}(\bar{\mathbf{P}} + \epsilon \Delta) - \partial_{\Delta} \mathcal{L}(\bar{\mathbf{P}})}{\epsilon} \geq 0.$$

Note that higher order directional derivatives are indeed well defined by continuity of the directional derivative **in the same direction**. Then, we need to investigate the directions Δ such that $\partial_{\Delta}^2 \mathcal{L}(\bar{\mathbf{P}}) = 0$, since the loss could increase, decrease or remain constant in those directions with higher orders. We will see that at order 3, these directions also yield $\partial_{\Delta}^3 \mathcal{L}(\bar{\mathbf{P}}) = 0$, and at order 4, necessarily, $\partial_{\Delta}^4 \mathcal{L}(\bar{\mathbf{P}}) \geq 0$, and since all higher order derivatives are null, this yields the claim.

This can be seen from the Taylor expansion of the loss in the direction Δ , which reads for small $\epsilon > 0$ as

$$\mathcal{L}(\bar{\mathbf{P}} + \epsilon \Delta) = \mathcal{L}(\bar{\mathbf{P}}) + \epsilon \partial_{\Delta} \mathcal{L}(\bar{\mathbf{P}}) + \frac{1}{2!} \epsilon^2 \partial_{\Delta}^2 \mathcal{L}(\bar{\mathbf{P}}) + \frac{1}{3!} \epsilon^3 \partial_{\Delta}^3 \mathcal{L}(\bar{\mathbf{P}}) + \frac{1}{4!} \epsilon^4 \partial_{\Delta}^4 \mathcal{L}(\bar{\mathbf{P}}).$$

F.1.1 Second-order Terms

We organize the Hessian matrix at $\bar{\mathbf{P}}$ correspondingly as:

$$H_{\mathcal{L}} = \begin{array}{c} \begin{array}{c} \overbrace{\left[\frac{\partial^2 \mathcal{L}(\bar{\mathbf{P}})}{\partial h_{j_1 i_1} \partial h_{j_2 i_2}} \right]}^{|I_h| \text{ columns}} \quad \overbrace{\left[\frac{\partial^2 \mathcal{L}(\bar{\mathbf{P}})}{\partial r_{i_1} \partial h_{j_2 i_2}} \right]}^{|I_r| \text{ columns}} \quad \overbrace{\left[\frac{\partial^2 \mathcal{L}(\bar{\mathbf{P}})}{\partial s_{i_1} \partial h_{j_2 i_2}} \right]}^{|I_s| \text{ columns}} \\ \left. \begin{array}{c} \left[\frac{\partial^2 \mathcal{L}(\bar{\mathbf{P}})}{\partial h_{j_1 i_1} \partial r_{i_2}} \right] \\ \left[\frac{\partial^2 \mathcal{L}(\bar{\mathbf{P}})}{\partial h_{j_1 i_1} \partial s_{i_2}} \right] \end{array} \right\} \begin{array}{c} |I_h| \text{ rows} \\ |I_r| \text{ rows} \\ |I_s| \text{ rows} \end{array} \end{array} \quad (7)$$

Computing the second order partial derivatives. Recall the first order partial derivatives

$$\begin{aligned} \frac{\partial \mathcal{L}(\mathbf{P})}{\partial h_{ji}} &= \sum_{k \in K} e_{kj} \rho(\mathbf{w}_i \cdot \mathbf{x}_k), \\ \frac{\partial \mathcal{L}(\mathbf{P})}{r_i} &= \sum_{j \in J} h_{ji} \sum_{k \in K} e_{kj} \rho(\mathbf{u}_i \cdot \mathbf{x}_k), \\ \frac{\partial \mathcal{L}(\mathbf{P})}{\partial s_i} &= \sum_{j \in J} h_{ji} \sum_{k \in K} e_{kj} \tilde{\rho}_{\mathbf{w}_i \cdot \mathbf{x}_k}(\mathbf{v}_i \cdot \mathbf{x}_k). \end{aligned}$$

We now compute the second-order derivatives of the loss. Recall that these derivatives are defined for fixed radial and tangential directions, that is, the vectors $\mathbf{u}_i, \mathbf{v}_i, i \in I$ are fixed. We have

$$\begin{aligned} \frac{\partial^2 \mathcal{L}(\mathbf{P})}{\partial h_{j_1 i_1} \partial h_{j_2 i_2}} &= \sum_{k \in K} \frac{\partial e_{kj_1}}{h_{j_2 i_2}} \rho(\mathbf{w}_i \cdot \mathbf{x}_k) \\ &= \sum_{k \in K} \mathbb{1}_{\{j_1=j_2\}} \rho(\mathbf{w}_{i_1} \cdot \mathbf{x}_k) \rho(\mathbf{w}_{i_2} \cdot \mathbf{x}_k), \\ \frac{\partial^2 \mathcal{L}(\mathbf{P})}{\partial r_{i_1} \partial h_{j_2 i_2}} &= \frac{\partial}{\partial h_{j_2 i_2}} \sum_{j' \in J} \sum_{k \in K} e_{kj'} h_{j' i_1} \rho(\mathbf{u}_{i_1} \cdot \mathbf{x}_k) \\ &= \sum_{k \in K} (e_{kj} \rho(\mathbf{u}_{i_1} \cdot \mathbf{x}_k) \mathbb{1}_{\{i_1=i_2\}} + h_{j i_1} \rho(\mathbf{u}_{i_1} \cdot \mathbf{x}_k) \rho(\mathbf{w}_{i_2} \cdot \mathbf{x}_k)), \\ \frac{\partial^2 \mathcal{L}(\mathbf{P})}{\partial s_{i_1} \partial h_{j_2 i_2}} &= \frac{\partial}{\partial h_{j_2 i_2}} h_{j i_1} \sum_{k \in K} e_{kj} \tilde{\rho}_{\mathbf{w}_{i_1} \cdot \mathbf{x}_k}(\mathbf{v}_{i_1} \cdot \mathbf{x}_k) \\ &= \sum_{k \in K} e_{kj} \tilde{\rho}_{\mathbf{w}_{i_1} \cdot \mathbf{x}_k}(\mathbf{v}_{i_1} \cdot \mathbf{x}_k) \mathbb{1}_{\{i_1=i_2\}} + h_{j i_1} \sum_{k \in K} \tilde{\rho}_{\mathbf{w}_{i_1} \cdot \mathbf{x}_k}(\mathbf{v}_{i_1} \cdot \mathbf{x}_k) \rho(\mathbf{w}_{i_2} \cdot \mathbf{x}_k), \\ \frac{\partial^2 \mathcal{L}(\mathbf{P})}{\partial r_{i_1} \partial r_{i_2}} &= \frac{\partial}{\partial r_2} \sum_{j \in J} \sum_{k \in K} e_{kj} h_{j i_1} \rho(\mathbf{u}_{i_1} \cdot \mathbf{x}_k) \\ &= \sum_{j \in J} \sum_{k \in K} h_{j i_1} h_{j i_2} \rho(\mathbf{u}_{i_1} \cdot \mathbf{x}_k) \rho(\mathbf{u}_{i_2} \cdot \mathbf{x}_k), \\ \frac{\partial^2 \mathcal{L}(\mathbf{P})}{\partial s_{i_1} \partial r_{i_2}} &= \frac{\partial}{\partial r_{i_2}} \sum_{j \in J} \sum_{k \in K} e_{kj} h_{j i_1} \tilde{\rho}_{\mathbf{w}_{i_1} \cdot \mathbf{x}_k}(\mathbf{v}_{i_1} \cdot \mathbf{x}_k) \\ &= \sum_{j \in J} \sum_{k \in K} h_{j i_1} h_{j i_2} \tilde{\rho}_{\mathbf{w}_{i_1} \cdot \mathbf{x}_k}(\mathbf{v}_{i_1} \cdot \mathbf{x}_k) \rho(\mathbf{u}_{i_2} \cdot \mathbf{x}_k), \\ \frac{\partial^2 \mathcal{L}(\mathbf{P})}{\partial s_{i_1} \partial s_{i_2}} &= \frac{\partial}{\partial s_{i_2}} \sum_{j \in J} \sum_{k \in K} e_{kj} h_{j i_1} \tilde{\rho}_{\mathbf{w}_{i_1} \cdot \mathbf{x}_k}(\mathbf{v}_{i_1} \cdot \mathbf{x}_k) \end{aligned}$$

$$= \sum_{j \in J} \sum_{k \in K} h_{ji_1} h_{ji_2} \tilde{\rho}_{\mathbf{w}_{i_1} \cdot \mathbf{x}_k}(\mathbf{v}_{i_1} \cdot \mathbf{x}_k) \tilde{\rho}_{\mathbf{w}_{i_2} \cdot \mathbf{x}_k}(\mathbf{v}_{i_2} \cdot \mathbf{x}_k)$$

Second order partial derivatives at the stationary point. When evaluated at the stationary point $\bar{\mathbf{P}}$, two of these derivatives simplify. Firstly, we note that, if $\|\mathbf{w}_i\| \neq 0$, then $\sum_{k \in K} (e_{kj} \rho(\mathbf{u}_{i_1} \cdot \mathbf{x}_k) \mathbb{1}_{\{i_1=i_2\}} = \frac{1}{\|\mathbf{w}_i\|} \frac{\partial \mathcal{L}(\bar{\mathbf{P}})}{\partial h_{ji_1}} = 0$ by stationarity. If $\|\mathbf{w}_i\| = 0$, $\|\mathbf{u}_i\| = 0$ by convention so the sum is null as well. In any case, we have that

$$\frac{\partial^2 \mathcal{L}(\bar{\mathbf{P}})}{\partial r_{i_1} \partial h_{ji_2}} = 0 + \sum_{k \in K} h_{ji_1} \rho(\mathbf{u}_{i_1} \cdot \mathbf{x}_k) \rho(\mathbf{w}_{i_2} \cdot \mathbf{x}_k).$$

Similarly, since we choose the direction Δ such that $\partial_{\Delta} \mathcal{L}(\bar{\mathbf{P}}) = 0$, we must have that $\frac{\partial \mathcal{L}(\bar{\mathbf{P}})}{\partial s_i} = 0$. Since there is no escape neuron, necessarily, $\sum_{k \in K} e_{kj} \tilde{\rho}_{\mathbf{w}_i \cdot \mathbf{x}_k}(\mathbf{v}_i \cdot \mathbf{x}_k) = \mathbf{d}_{ji}^{\mathbf{v}_i} \cdot \mathbf{v}_i = 0$. This implies that

$$\frac{\partial^2 \mathcal{L}(\mathbf{P})}{\partial s_{i_1} \partial h_{ji_2}} = 0 + h_{ji_1} \sum_{k \in K} \tilde{\rho}_{\mathbf{w}_{i_1} \cdot \mathbf{x}_k}(\mathbf{v}_{i_1} \cdot \mathbf{x}_k) \rho(\mathbf{w}_{i_2} \cdot \mathbf{x}_k). \quad (8)$$

The Hessian matrix is positive semidefinite. Define the following three $|K|$ -dimensional vectors: for $i \in I, j \in J$, let

$$\mathbf{V}_{h_{ji}} := (\rho(\mathbf{w}_i \cdot \mathbf{x}_k))_{k=1, \dots, |K|}, \quad (9)$$

$$\mathbf{V}_{r_i}^j := (h_{ji} \rho(\mathbf{u}_i \cdot \mathbf{x}_k))_{k=1, \dots, |K|}, \quad (10)$$

$$\mathbf{V}_{s_i}^j := (h_{ji} \tilde{\rho}_{\mathbf{w}_i \cdot \mathbf{x}_k}(\mathbf{v}_i \cdot \mathbf{x}_k))_{k=1, \dots, |K|}. \quad (11)$$

Then, we assemble the vectors and for $j' \in J$, we define the matrix

$$V_{j'} := \left((\mathbb{1}_{\{j=j'\}} \mathbf{V}_{h_{ji}})_{(j,i) \in I_h}, (\mathbf{V}_{r_i}^{j'})_{i \in I_r}, (\mathbf{V}_{s_i}^{j'})_{i \in I_s} \right) \in \mathbb{R}^{|K| \times D'},$$

where $\mathbb{1}_{\{j=j'\}}$ is multiplied to each component of $\mathbf{V}_{h_{ji}}$. The vectors are disposed such that each is a column of $V_{j'}$. We thus see that the directional Hessian (7) can be written as

$$\mathcal{H}_{\mathcal{L}} = \sum_{j' \in J} V_{j'}^{\top} V_{j'}. \quad (12)$$

Once again, like the vectors $\mathbf{u}_i, \mathbf{v}_i$ for $i \in I$, the Hessian matrix implicitly depends on the direction Δ . Hence, for every fixed unit vector $\Delta \in \mathbb{R}^D$, the Hessian matrix $\mathcal{H}_{\mathcal{L}}$ is a sum of positive semidefinite Gram matrices, and as such, is positive semidefinite.

We deduce that for all unit vector $\Delta \in \mathbb{R}^D$, it holds that

$$\partial_{\Delta}^2 \mathcal{L}(\bar{\mathbf{P}}) = \Delta^{\top} \mathcal{H}_{\mathcal{L}} \Delta \geq 0,$$

as claimed.

F.1.2 Third-order Terms

In this section, we continue our reasoning and assume that $\bar{\mathbf{P}}$ is a stationary point with no escape neuron and $\Delta \in \mathbb{R}^D$ is a fixed unitary vector such that $\partial_{\Delta}^2 \mathcal{L}(\bar{\mathbf{P}}) = \Delta^{\top} \mathcal{H}_{\mathcal{L}} \Delta = 0$. In particular, since $\mathcal{H}_{\mathcal{L}} = \sum_{j \in J} V_j^{\top} V_j$ in this case, it holds that $V_j \Delta \in \mathbb{R}^{|K|}$ is a zero vector for all $j \in J$, where V_j is defined below (9). We show below that this entails $\partial_{\Delta}^3 \mathcal{L}(\bar{\mathbf{P}}) = 0$.

From the formulas for the second-order terms, we can see that there can only be six types of non-zero third-order derivatives, namely, $\frac{\partial^3 \mathcal{L}(\bar{\mathbf{P}})}{\partial h_{ji_1} \partial r_{i_1} \partial h_{ji_2}}$, $\frac{\partial^3 \mathcal{L}(\bar{\mathbf{P}})}{\partial h_{ji_1} \partial r_{i_1} \partial r_{i_2}}$, $\frac{\partial^3 \mathcal{L}(\bar{\mathbf{P}})}{\partial h_{ji_1} \partial r_{i_1} \partial s_{i_2}}$, $\frac{\partial^3 \mathcal{L}(\bar{\mathbf{P}})}{\partial h_{ji_1} \partial s_{i_1} \partial h_{ji_2}}$, $\frac{\partial^3 \mathcal{L}(\bar{\mathbf{P}})}{\partial h_{ji_1} \partial s_{i_1} \partial r_{i_2}}$, and $\frac{\partial^3 \mathcal{L}(\bar{\mathbf{P}})}{\partial h_{ji_1} \partial s_{i_1} \partial s_{i_2}}$.

Recall the vectors $\mathbf{V}_{h_{ji}}^{j'}$, $\mathbf{V}_{r_i}^{j'}$, $\mathbf{V}_{s_i}^{j'}$ defined in (9), and defined the following vectors

$$\mathbf{V}_{hr_i} = (\rho(\mathbf{u}_i \cdot \mathbf{x}_k))_{k \in \{1, 2, \dots, K\}},$$

$$\mathbf{V}_{hs_i} = (\tilde{\rho}_{\mathbf{w}_i \cdot \mathbf{x}_k}(\mathbf{v}_i \cdot \mathbf{x}_k))_{k \in \{1, 2, \dots, K\}},$$

The third order partial derivatives can be conveniently expressed using them. For example, we compute the first one

$$\begin{aligned} \frac{\partial^3 \mathcal{L}(\bar{\mathbf{P}})}{\partial h_{ji_1} \partial r_{i_1} \partial h_{ji_2}} &= \frac{\partial}{\partial h_{ji_2}} \sum_{k \in K} (e_{kj} \rho(\mathbf{u}_{i_1} \cdot \mathbf{x}_k) + h_{ji_1} \rho(\mathbf{u}_{i_1} \cdot \mathbf{x}_k) \rho(\mathbf{w}_{i_1} \cdot \mathbf{x}_k)) \\ &= (1 + \mathbb{1}_{\{i_1=i_2\}}) \sum_{k \in K} \rho(\mathbf{u}_{i_1} \cdot \mathbf{x}_k) \rho(\mathbf{w}_{i_2} \cdot \mathbf{x}_k) \\ &= (1 + \mathbb{1}_{\{i_1=i_2\}}) \mathbf{V}_{hr_{i_1}} \cdot \mathbf{V}_{h_{ji_2}}. \end{aligned}$$

The other derivatives follow similar easy calculations that are left to the reader, yielding the following results:

$$\begin{aligned} \frac{\partial^3 \mathcal{L}(\bar{\mathbf{P}})}{\partial h_{ji_1} \partial r_{i_1} \partial r_{i_2}} &= (1 + \mathbb{1}_{\{i_1=i_2\}}) \mathbf{V}_{hr_{i_1}} \cdot \mathbf{V}_{r_{i_2}}^j \\ \frac{\partial^3 \mathcal{L}(\bar{\mathbf{P}})}{\partial h_{ji_1} \partial r_{i_1} \partial s_{i_2}} &= (1 + \mathbb{1}_{\{i_1=i_2\}}) \mathbf{V}_{hr_{i_1}} \cdot \mathbf{V}_{s_{i_2}}^j \\ \frac{\partial^3 \mathcal{L}(\bar{\mathbf{P}})}{\partial h_{ji_1} \partial s_{i_1} \partial h_{ji_2}} &= (1 + \mathbb{1}_{\{i_1=i_2\}}) \mathbf{V}_{hs_{i_1}} \cdot \mathbf{V}_{h_{ji_2}} \\ \frac{\partial^3 \mathcal{L}(\bar{\mathbf{P}})}{\partial h_{ji_1} \partial s_{i_1} \partial r_{i_2}} &= (1 + \mathbb{1}_{\{i_1=i_2\}}) \mathbf{V}_{hs_{i_1}} \cdot \mathbf{V}_{r_{i_2}}^j \\ \frac{\partial^3 \mathcal{L}(\bar{\mathbf{P}})}{\partial h_{ji_1} \partial s_{i_1} \partial s_{i_2}} &= (1 + \mathbb{1}_{\{i_1=i_2\}}) \mathbf{V}_{hs_{i_1}} \cdot \mathbf{V}_{s_{i_2}}^j. \end{aligned}$$

In the third order directional derivative of the loss at $\bar{\mathbf{P}}$ in direction Δ , each of the above derivatives appear. More specifically, if $i_1 \neq i_2$, then any of them is counted $3! = 6$ times (the number of orderings that yield the same derivative) and if $i_1 = i_2$, then it is counted 3 times. We thus see that

$$\begin{aligned} \partial_{\Delta}^3 \mathcal{L}(\bar{\mathbf{P}}) &= \sum_{j \in J} \left(6 \sum_{i_1 \neq i_2 \in I} \Delta_{h_{ji_1}} \Delta_{r_{i_1}} \mathbf{V}_{hr_{i_1}} (\Delta_{h_{ji_2}} V_{h_{ji_2}} + \Delta_{r_{i_2}} V_{r_{i_2}} + \Delta_{s_{i_2}} V_{s_{i_2}}) \right. \\ &\quad \left. + 2 \times 3 \sum_{i_1 \in I} \Delta_{h_{ji_1}} \Delta_{r_{i_1}} \mathbf{V}_{hr_{i_1}} (\Delta_{h_{ji_1}} V_{h_{ji_1}} + \Delta_{r_{i_1}} V_{r_{i_1}} + \Delta_{s_{i_1}} V_{s_{i_1}}) \right) \\ &\quad + \sum_{j \in J} \left(6 \sum_{i_1 \neq i_2 \in I} \Delta_{h_{ji_1}} \Delta_{s_{i_1}} \mathbf{V}_{hs_{i_1}} (\Delta_{h_{ji_2}} V_{h_{ji_2}} + \Delta_{r_{i_2}} V_{r_{i_2}} + \Delta_{s_{i_2}} V_{s_{i_2}}) \right. \\ &\quad \left. + 2 \times 3 \sum_{i_1 \in I} \Delta_{h_{ji_1}} \Delta_{s_{i_1}} \mathbf{V}_{hs_{i_1}} (\Delta_{h_{ji_1}} V_{h_{ji_1}} + \Delta_{r_{i_1}} V_{r_{i_1}} + \Delta_{s_{i_1}} V_{s_{i_1}}) \right) \\ &= 6 \sum_{j \in J} \sum_{i_1, i_2 \in I} \Delta_{h_{ji_1}} (\Delta_{r_{i_1}} \mathbf{V}_{hr_{i_1}} + \Delta_{s_{i_1}} \mathbf{V}_{hs_{i_1}}) V_j \Delta \end{aligned}$$

Recall from the discussion at the start of the subsection that since $\bar{\mathbf{P}}$ is a stationary point with no escape neuron and since $\partial_{\Delta}^2 \mathcal{L}(\bar{\mathbf{P}}) = 0$, it holds that

$$V_j \Delta = 0. \tag{13}$$

This shows that $\partial_{\Delta}^3 \mathcal{L}(\bar{\mathbf{P}}) = 0$, as claimed.

F.1.3 Fourth-order Terms

This is the last step of our argument, where we show that $\partial_{\Delta}^4 \mathcal{L}(\bar{\mathbf{P}}) \geq 0$ always holds.

We compute the fourth-order partial derivatives of the loss. Note from the third order partial derivatives that only three of them can be non null, namely $\frac{\partial^4 \mathcal{L}(\bar{\mathbf{P}})}{\partial h_{ji_1} \partial r_{i_1} \partial h_{ji_2} \partial r_{i_2}}, \frac{\partial^4 \mathcal{L}(\bar{\mathbf{P}})}{\partial h_{ji_1} \partial s_{i_1} \partial h_{ji_2} \partial s_{i_2}}$

and $\frac{\partial^4 \mathcal{L}(\bar{\mathbf{P}})}{\partial h_{ji_1} \partial r_{i_1} \partial h_{ji_2} \partial s_{i_2}}$. It is straightforward – but cumbersome therefore left to the reader – to check the following:

$$\begin{aligned}\frac{\partial^4 \mathcal{L}(\bar{\mathbf{P}})}{\partial h_{ji_1} \partial r_{i_1} \partial h_{ji_2} \partial r_{i_2}} &= (1 + \mathbb{1}_{\{i_1=i_2\}}) \mathbf{V}_{hr_{i_1}} \cdot \mathbf{V}_{hr_{i_2}} \\ \frac{\partial^4 \mathcal{L}(\bar{\mathbf{P}})}{\partial h_{ji_1} \partial s_{i_1} \partial h_{ji_2} \partial s_{i_2}} &= (1 + \mathbb{1}_{\{i_1=i_2\}}) \mathbf{V}_{hs_{i_1}} \cdot \mathbf{V}_{hs_{i_2}}, \\ \frac{\partial^4 \mathcal{L}(\bar{\mathbf{P}})}{\partial h_{ji_1} \partial r_{i_1} \partial h_{ji_2} \partial s_{i_2}} &= (1 + \mathbb{1}_{\{i_1=i_2\}}) \mathbf{V}_{hr_{i_1}} \cdot \mathbf{V}_{hs_{i_2}}.\end{aligned}$$

As for the third order, depending on whether i_1 equals i_2 , the number of occurrences of these derivatives changes between $4!$ and $4!/2$, and the fourth order directional derivative reads as

$$\begin{aligned}\partial_{\Delta}^4 \mathcal{L}(\bar{\mathbf{P}}) &= \sum_{j \in J} \left(\sum_{i_1 \neq i_2 \in I} 4! \Delta_{h_{ji_1}} \Delta_{r_{i_1}} \Delta_{h_{ji_2}} \Delta_{r_{i_2}} \mathbf{V}_{hr_{i_1}} \cdot \mathbf{V}_{hr_{i_2}} + \sum_{i_1 \in I} 2 \frac{4!}{2 \times 2} \Delta_{h_{ji_1}}^2 \Delta_{r_{i_1}}^2 \mathbf{V}_{hr_{i_1}} \cdot \mathbf{V}_{hr_{i_1}} \right) \\ &\quad + \sum_{j \in J} \left(\sum_{i_1 \neq i_2 \in I} 4! \Delta_{h_{ji_1}} \Delta_{s_{i_1}} \Delta_{h_{ji_2}} \Delta_{s_{i_2}} \mathbf{V}_{hs_{i_1}} \cdot \mathbf{V}_{hs_{i_2}} + \sum_{i_1 \in I} 2 \frac{4!}{2 \times 2} \Delta_{h_{ji_1}}^2 \Delta_{s_{i_1}}^2 \mathbf{V}_{hs_{i_1}} \cdot \mathbf{V}_{hs_{i_1}} \right) \\ &\quad + \sum_{j \in J} \left(\sum_{i_1 \neq i_2 \in I} 4! \Delta_{h_{ji_1}} \Delta_{r_{i_1}} \Delta_{h_{ji_2}} \Delta_{s_{i_2}} \mathbf{V}_{hr_{i_1}} \cdot \mathbf{V}_{hs_{i_2}} + \sum_{i_1 \in I} 2 \frac{4!}{2} \Delta_{h_{ji_1}}^2 \Delta_{r_{i_1}} \Delta_{s_{i_1}} \mathbf{V}_{hr_{i_1}} \cdot \mathbf{V}_{hs_{i_1}} \right) \\ &= \frac{4!}{2} \sum_{j \in J} \left(\sum_{i_1, i_2 \in I} \Delta_{h_{ji_1}} \Delta_{r_{i_1}} \Delta_{h_{ji_2}} \Delta_{r_{i_2}} \mathbf{V}_{hr_{i_1}} \cdot \mathbf{V}_{hr_{i_2}} + \Delta_{h_{ji_1}} \Delta_{s_{i_1}} \Delta_{h_{ji_2}} \Delta_{s_{i_2}} \mathbf{V}_{hs_{i_1}} \cdot \mathbf{V}_{hs_{i_2}} \right. \\ &\quad \left. + 2 \Delta_{h_{ji_1}} \Delta_{r_{i_1}} \Delta_{h_{ji_2}} \Delta_{s_{i_2}} \mathbf{V}_{hr_{i_1}} \cdot \mathbf{V}_{hs_{i_2}} \right) \\ &= \frac{4!}{2} \sum_{j \in J} \left(\sum_{i_1, i_2 \in I} (\Delta_{h_{ji_1}} \Delta_{r_{i_1}} \mathbf{V}_{hr_{i_1}} + \Delta_{h_{ji_1}} \Delta_{s_{i_1}} \mathbf{V}_{hs_{i_1}}) \cdot (\Delta_{h_{ji_2}} \Delta_{r_{i_2}} \mathbf{V}_{hr_{i_2}} + \Delta_{h_{ji_2}} \Delta_{s_{i_2}} \mathbf{V}_{hs_{i_2}}) \right) \\ &= \frac{4!}{2} \sum_{j \in J} \bar{\mathbf{V}}_j^T \bar{\mathbf{V}}_j,\end{aligned}$$

where we just introduced the vector $\bar{\mathbf{V}}_j$, defined by

$$\left(\sum_{i \in I} \Delta_{h_{ji}} \Delta_{r_i} \mathbf{V}_{hr_i} + \Delta_{h_{ji}} \Delta_{s_i} \mathbf{V}_{hs_i} \right)_{j \in J}.$$

We see from the above that $\partial_{\Delta} \mathcal{L}(\bar{\mathbf{P}}) \geq 0$, as claimed, which concludes the proof of the sufficiency in Theorem 4.2.

Remark F.1 (about Corollary 4.7). Note, at a stationary point, if a perturbation direction Δ does not perturb the parameters of escape neurons, then the above proof also effectively shows that such a perturbation can not strictly decrease the loss, which gives rise to Corollary 4.7.

F.2 Proof of the Necessity in Theorem 4.2

The necessity of the condition in Theorem 4.2, which holds in the scalar-output case, will be proved in the following via contradiction. Namely, if $\bar{\mathbf{P}}$ is a stationary point on the loss landscape with at least one hidden neuron being an escape neuron, then this stationary point cannot be a local minimum. Let us select one such hidden neuron i , associated with $(\bar{h}_{j_0 i}$ and $\bar{\mathbf{w}}_i)$. To construct the loss-decreasing path, we perturb $\bar{h}_{j_0 i}$ and $\bar{\mathbf{w}}_i$ with $\Delta h_{j_0 i}$ and $\Delta \mathbf{w}_i = \Delta s_i \mathbf{v}_i$, respectively; \mathbf{v}_i being one of the tangential directions satisfying and $\frac{\partial \mathcal{L}(\bar{\mathbf{P}})}{\partial s_i} = 0$ and $\mathbf{d}_{j_0 i}^{\mathbf{v}_i} \cdot \mathbf{v}_i \neq 0$. We assert that we can design the following perturbation to strictly decrease the loss: $\Delta h_{ji} = -\text{sgn}(\mathbf{d}_{j_0 i}^{\mathbf{v}_i} \cdot \mathbf{v}_i) a$, $\Delta s_i = b$, with $a, b > 0$ sufficiently small and satisfying certain conditions, which is discussed below.

To study the loss change after perturbing the weights as described, we resort to Taylor expansion again. In this case, we only need to look into terms of no higher than the second order.

For the first-order terms, we have:

$$T_1(\bar{\mathbf{P}}, \Delta \mathbf{P}') = \frac{\partial \mathcal{L}(\bar{\mathbf{P}})}{\partial h_{j_0 i}} \Delta h_{j_0 i} + \frac{\partial \mathcal{L}(\bar{\mathbf{P}})}{\partial s_i} \Delta s_i. \quad (14)$$

Since $\bar{\mathbf{P}}$ is a stationary point, we must have $\frac{\partial \mathcal{L}(\bar{\mathbf{P}})}{\partial h_{j_0 i}} = 0$. Moreover, we have $\frac{\partial \mathcal{L}(\bar{\mathbf{P}})}{\partial s_i} = 0$, as this is how we choose the tangential perturbation direction \mathbf{v}_i . Thus we have $T_1(\bar{\mathbf{P}}, \Delta \mathbf{P}') = 0$.

Then we calculate the second-order terms. Three types of second-order derivatives are involved, $\frac{\partial^2 \mathcal{L}(\bar{\mathbf{P}})}{\partial h_{j_0 i}^2}$, $\frac{\partial^2 \mathcal{L}(\bar{\mathbf{P}})}{\partial s_i^2}$, and $\frac{\partial^2 \mathcal{L}(\bar{\mathbf{P}})}{\partial h_{j_0 i} \partial s_i}$. Notice that, in Equation (8), we could simplify the last derivative given that the neuron is not an escape neuron, which we can no longer do here. This causes the Hessian matrix to be indefinite.

Notice that, we must also have $\bar{h}_{j_0 i} = 0$ to fulfill the requirements of an escape neuron in the scalar output case. Hence, we have $\mathbf{V}_{s_i}^{j_0} = 0$. Thus, the second-order terms can be derived as:

$$T_2(\bar{\mathbf{P}}, \Delta \mathbf{P}') = \frac{\partial^2 \mathcal{L}(\bar{\mathbf{P}})}{\partial h_{j_0 i}^2} (\Delta h_{j_0 i})^2 + \frac{\partial^2 \mathcal{L}(\bar{\mathbf{P}})}{\partial s_i^2} (\Delta s_i)^2 + 2 \frac{\partial^2 \mathcal{L}(\bar{\mathbf{P}})}{\partial h_{j_0 i} \partial s_i} \Delta h_{j_0 i} \Delta s_i \quad (15a)$$

$$= \mathbf{V}_{h_{j_0 i}} \cdot \mathbf{V}_{h_{j_0 i}} (\Delta h_{j_0 i})^2 + \underbrace{\mathbf{V}_{s_i}^{j_0} \cdot \mathbf{V}_{s_i}^{j_0}}_{(=0)} (\Delta s_i)^2 + 2(\mathbf{d}_{j_0 i}^{\mathbf{v}} \cdot \mathbf{v}_i + \mathbf{V}_{h_{j_0 i}} \cdot \underbrace{\mathbf{V}_{s_i}^{j_0}}_{(=0)}) \Delta h_{j_0 i} \Delta s_i \quad (15b)$$

$$= \|\mathbf{V}_{h_{j_0 i}}\|^2 a^2 + 2(\mathbf{d}_{j_0 i}^{\mathbf{v}_i} \cdot \mathbf{v}_i) (-\text{sgn}(\mathbf{d}_{j_0 i}^{\mathbf{v}_i} \cdot \mathbf{v}_i)) ab \quad (15c)$$

$$= \|\mathbf{V}_{h_{j_0 i}}\|^2 a^2 - 2|\mathbf{d}_{j_0 i}^{\mathbf{v}_i} \cdot \mathbf{v}_i| ab \quad (15d)$$

Note, we have specified that both a and b are positive. Thus, if we choose these two numbers such that:

$$b > \frac{\|\mathbf{V}_{h_{j_0 i}}\|^2}{2|\mathbf{d}_{j_0 i}^{\mathbf{v}_i} \cdot \mathbf{v}_i|} a. \quad (16)$$

Then we have $T_2(\bar{\mathbf{P}}, \Delta \mathbf{P}')$ being strictly negative, indicating a strictly loss-decreasing path, which completes the proof.

Remark F.2 (about Corollary 4.4). When we perturb the parameters of the escape neurons as above, we are exploiting second-order loss-decreasing paths, which yields the statement of Corollary 4.4.

F.2.1 Why cannot we prove the necessity for networks with multiple output neurons?

The construction of the loss-decreasing path in this section is based on the observation that the Hessian matrix is no longer a positive semi-definite matrix when there exist escape neurons for $|J| = 1$ case. However, in the case where $|J| > 1$, we cannot draw a similar conclusion. When the network has multiple output neurons, there is currently no guarantee that escape neurons will introduce negative eigenvalues in the Hessian matrix. More specifically, like the $|J| = 1$ case, some $\frac{\partial^2 \mathcal{L}(\bar{\mathbf{P}})}{\partial s_i \partial h_{j_i}}$ term in the Hessian matrix is no longer simply a dot product of two vectors, $\mathbf{V}_{s_i}^{j_i} \cdot \mathbf{V}_{h_{j_i}}$, but is added with a non-zero term of $\mathbf{d}_{j_i}^{\mathbf{v}_i} \cdot \mathbf{v}_i$. Owing to this, we can no longer write the Hessian matrix as a sum of Gram matrices as in Equation (12). Nonetheless, this does not necessarily mean that the Hessian matrix admits negative eigenvalues, which is why the necessity in Theorem 4.2 does not hold for general cases.

More concretely, the Hessian matrix for a multidimensional output network at a stationary point with escape neurons can be denoted as:

$$H_{\mathcal{L}} = \sum_{j \in J} \underbrace{(\tilde{H}_j + \mathbf{V}_j^{\top} \mathbf{V}_j)}_{\text{defined to be } H_{\mathcal{L}}^j} \quad (17)$$

Compared with Equation (12), Equation (17) has an extra term (\tilde{H}_j) in the summation which contains the terms of $\mathbf{d}_{j_i}^{\mathbf{v}_i} \cdot \mathbf{v}_i \neq 0$ at the positions held by $\frac{\partial^2 \mathcal{L}(\bar{\mathbf{P}})}{\partial h_{j_i} \partial s_i}$ or $\frac{\partial^2 \mathcal{L}(\bar{\mathbf{P}})}{\partial s_i \partial h_{j_i}}$ in the Hessian matrix. It is easy to see that $H_{\mathcal{L}}^j$ is not positive semi-definite as long as \tilde{H}_j is not a zero matrix.

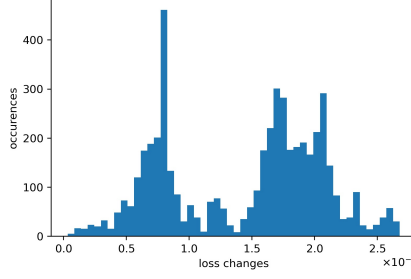


Figure 10: An occurrence histogram showing the loss changes incurred by the 5000 perturbations.

Consequently, if the sufficient condition in Theorem 4.2 is not satisfied, then the Hessian matrix constructed based on the perturbation becomes a summation of matrices, some of which are indefinite. However, there can be no theoretical guarantee that such a summation cannot lead to a positive semi-definite matrix in the end. Thus, even if the sufficient condition in Theorem 4.2 is violated, the Hessian matrix may still be positive semi-definite. *However, despite the possibility of this case, the chance of a summation of indefinite matrices and positive semidefinite matrices resulting in a positive semidefinite matrix is relatively small. Even if the Hessian matrix is positive semidefinite, the existence of escape neurons seems to hinder us from claiming anything general regarding the loss change incurred by the third-order terms.*⁴ This is because our current discussion regarding the third-order terms (in Appendix F.1.2) relies on the description of the flat directions in the second-order terms being Equation (13), which is premised on the absence of escape neurons. Hence, we believe that local minima contradicting the sufficient condition of Theorem 4.2 (the so-called type-2 local minima) should be rare if exist. The rigorous characterization regarding the "rarity" will be conducted in the future.

G Verifying Local Minimality in a Real Case

The fact that the last long plateau in Figure 3a corresponds to a local minimum can be verified with a numerical experiment. The verification can be conducted by perturbing the parameters at the end of the training with small noises and investigating whether such perturbations yield negative loss change. In our experiment, we perturb all the parameters by adding noise to all of them. The noise added to each of the parameters is independently generated from a zero-centered uniform distribution $\mathcal{U}(-\zeta, \zeta)$, where $\zeta > 0$ is a small value making sure that the network parameters after perturbation still stays in its neighborhood. Namely, the loss function restricted on the line segment connecting the parameters before and after the perturbation should be C^∞ , meaning the line segment should not stretch across a non-differentiable area in the parameter space. In our case, we chose $\zeta \approx 1.28 \times 10^{-4}$. We conducted the perturbation for 5000 times and recorded the loss change incurred by each perturbation, which is illustrated in a frequency histogram in Figure 10. One can see that all of the perturbations resulted in positive loss change, agreeing with our theoretical prediction.

H Proof of Proposition 4.8

H.1 Conditions for Unit Replication to Preserve Stationarity

Let us denote the parameters of the stationary point before unit replication by $\bar{\mathbf{P}}$ and the parameters after by $\bar{\mathbf{P}}'$. Then, Definition 3.3 dictates that $\bar{\mathbf{P}}$ must satisfy:

$$\left. \frac{\partial \mathcal{L}(\mathbf{P})}{\partial h_{ji}} \right|_{\mathbf{P}=\bar{\mathbf{P}}} = 0, \quad \forall j \in J, i \in I; \quad (18a)$$

$$\left. \frac{\partial \mathcal{L}(\mathbf{P})}{\partial r_i} \right|_{\mathbf{P}=\bar{\mathbf{P}}} = 0, \quad \forall i \in I; \quad (18b)$$

⁴Note that the fourth-order terms always lead to non-negative loss changes, as shown in Appendix F.1.3

$$\left. \frac{\partial \mathcal{L}(\mathbf{P})}{\partial s_i} \right|_{\mathbf{P}=\bar{\mathbf{P}}} \geq 0, \forall i \in I, \forall \text{ tangential direction } \mathbf{v}_i \text{ of } \bar{\mathbf{w}}_i. \quad (18c)$$

It is easy to check that, after unit replication, the above still holds for the hidden neurons within the set $I \setminus \{i_0\}$, which are the hidden neurons untouched by unit replication, since the network function is not changed by this process. For the rest of the hidden neurons in $\bar{\mathbf{P}}'$, which are indexed by $i_0^l \in L$, we can also deduce whether they conform to the conditions for stationarity. We have the following:

$$\left. \frac{\partial \mathcal{L}(\mathbf{P})}{\partial h_{ji_0^l}} \right|_{\mathbf{P}=\bar{\mathbf{P}}'} = \mathbf{w}_{i_0^l} \cdot \mathbf{d}_{ji_0^l} = \beta_l \mathbf{w}_{i_0} \cdot \mathbf{d}_{ji_0} = \beta_l \left. \frac{\partial \mathcal{L}(\mathbf{P})}{\partial h_{ji_0}} \right|_{\mathbf{P}=\bar{\mathbf{P}}} = 0. \quad (19)$$

If $\|\mathbf{w}_{i_0^l}\| = \beta_l \|\mathbf{w}_{i_0}\| > 0$, then the newly generated hidden neurons have radial directions:

$$\left. \frac{\partial \mathcal{L}(\mathbf{P})}{\partial r_{i_0^l}} \right|_{\mathbf{P}=\bar{\mathbf{P}}'} = \sum_{j \in J} h_{ji_0^l} \mathbf{d}_{ji_0^l} \cdot \mathbf{u}_{i_0^l} = \gamma_l \sum_{j \in J} h_{ji_0} \mathbf{d}_{ji_0} \cdot \mathbf{u}_{i_0} = \gamma_l \underbrace{\left. \frac{\partial \mathcal{L}(\mathbf{P})}{\partial r_{i_0}} \right|_{\mathbf{P}=\bar{\mathbf{P}}}}_{(=0)} = 0. \quad (20)$$

If $\|\mathbf{w}_{i_0^l}\| = \beta_l \|\mathbf{w}_{i_0}\| = 0$, then, by convention, the radial derivative $\left. \frac{\partial \mathcal{L}(\mathbf{P})}{\partial r_{i_0^l}} \right|_{\bar{\mathbf{P}}'}$ are set to zero without loss of rigor.

As for the tangential derivatives of the newly generated hidden neurons, we have:

$$\left. \frac{\partial \mathcal{L}(\mathbf{P})}{\partial s_{i_0^l}} \right|_{\mathbf{P}=\bar{\mathbf{P}}'} = \sum_{j \in J} h_{ji_0^l} \mathbf{d}_{ji_0^l} \cdot \mathbf{v}_{i_0^l} = \gamma_l \sum_{j \in J} h_{ji_0} \mathbf{d}_{ji_0} \cdot \mathbf{v}_{i_0} = \gamma_l \underbrace{\left. \frac{\partial \mathcal{L}(\mathbf{P})}{\partial s_{i_0}} \right|_{\mathbf{P}=\bar{\mathbf{P}}}}_{(\geq 0)}, \quad (21)$$

where we take $\mathbf{v}_{i_0^l} = \mathbf{v}_{i_0}$. Namely, we are implying that any tangential direction of $\mathbf{w}_{i_0^l}$ must also be a tangential direction of \mathbf{w}_{i_0} . This is justified by the fact that $\beta_l > 0, \forall l \in L$.

With the above, we can infer $\left. \frac{\partial \mathcal{L}(\mathbf{P})}{\partial s_{i_0^l}} \right|_{\mathbf{P}=\bar{\mathbf{P}}'} \geq 0$ for all possible tangential direction $\mathbf{v}_{i_0^l}$'s if and only if either of the following is true:

1. $\left. \frac{\partial \mathcal{L}(\bar{\mathbf{P}})}{\partial s_{i_0}} \right| = 0, \forall \text{ tangential direction } \mathbf{v}_{i_0} \text{ of } \mathbf{w}_{i_0},$
2. $\gamma_l \geq 0, \forall l \in L;$

which concludes the proof.

H.2 Conditions for Unit Replication to Preserve Type-1 Local Minimality

The necessary and sufficient condition to preserve type-1 local minimality after unit replication is to avoid generating escape neurons and to preserve conditions for stationarity. Thus, we prove Lemma 4.8 by seeking necessary and sufficient conditions to achieve both these two goals. Let us denote the parameters of the stationary point before unit replication by $\bar{\mathbf{P}}$ and the parameters after by $\bar{\mathbf{P}}'$.

H.2.1 Avoid Generating escape neurons

First, let us consider two unit replication schemes:

1. (*replicate a tangentially flat hidden neuron*) Choose to replicate a hidden neuron i_0 satisfying $\left. \frac{\partial \mathcal{L}(\mathbf{P})}{\partial s_{i_0}} \right|_{\mathbf{P}=\bar{\mathbf{P}}} = 0$, for all tangential direction \mathbf{v}_{i_0} 's.
2. (*replicate with active propagation*) Let $\gamma_l \neq 0, \forall l \in L$.

Proposition H.1. *Unit replication process conforming to at least one of the two methods is sufficient and necessary for avoiding escape neurons.*

Proof.

Sufficiency:

Let us discuss the first way, replicating a tangentially flat hidden neuron. Since we have:

$$\left. \frac{\partial \mathcal{L}(\mathbf{P})}{\partial s_{i_0}} \right|_{\mathbf{P}=\bar{\mathbf{P}}} = \sum_{j \in J} \bar{h}_{ji_0} \mathbf{d}_{ji_0}^{\mathbf{v}_{i_0}} \cdot \mathbf{v}_{i_0} = 0, \quad \forall \text{ tangential direction } \mathbf{v}_{i_0} \text{ of } \bar{\mathbf{w}}_{i_0}. \quad (22)$$

Based on the definition of type-1 local minima, we know that:

$$\mathbf{d}_{ji_0}^{\mathbf{v}_{i_0}} \cdot \mathbf{v}_{i_0} = 0, \quad \forall j \in J, \forall \text{ tangential direction } \mathbf{v}_{i_0} \text{ of } \bar{\mathbf{w}}_{i_0}. \quad (23)$$

After unit replication, we have: For all $l \in L$, (1) $\mathbf{d}_{ji_0}^{\mathbf{v}_{i_0}^l} = \mathbf{d}_{ji_0}^{\mathbf{v}_{i_0}}$, $\forall j \in J$, for all tangential direction \mathbf{v}_{i_0} of $\bar{\mathbf{w}}_{i_0}$; (2) $\bar{\mathbf{w}}_{i_0}^l = \beta_l \bar{\mathbf{w}}_{i_0}$ with $\beta_l > 0$, which means any tangential direction of $\bar{\mathbf{w}}_{i_0}^l$ are also a tangential direction of $\bar{\mathbf{w}}_{i_0}$. These, combined with Equation (23), leads to:

$$\mathbf{d}_{ji_0}^{\mathbf{v}_{i_0}^l} \cdot \mathbf{v}_{i_0}^l = 0, \quad \forall l \in L, \forall j \in J, \forall \text{ tangential direction } \mathbf{v}_{i_0}^l \text{ of } \bar{\mathbf{w}}_{i_0}^l. \quad (24)$$

According to Definition 4.1, such i_0^l cannot be escape neurons.

Next, let us discuss the second way, replicating with active propagation. If the replicated hidden neuron is a tangentially flat hidden neuron, then the discussion above will already guarantee that the unit replication process does not introduce escape neurons. Thus, we only need to focus on the following type of neurons:

$$\left. \frac{\partial \mathcal{L}(\mathbf{P})}{\partial s_{i_0}} \right|_{\mathbf{P}=\bar{\mathbf{P}}} = \sum_{j \in J} \bar{h}_{ji_0} \mathbf{d}_{ji_0}^{\mathbf{v}_{i_0}} \cdot \mathbf{v}_{i_0} > 0, \quad \text{for some tangential direction } \mathbf{v}_{i_0} \text{ of } \bar{\mathbf{w}}_{i_0}. \quad (25)$$

In this case, for any direction \mathbf{v}_{i_0} with $\left. \frac{\partial \mathcal{L}(\mathbf{P})}{\partial s_{i_0}} \right|_{\mathbf{P}=\bar{\mathbf{P}}} = \sum_{j \in J} \bar{h}_{ji_0} \mathbf{d}_{ji_0}^{\mathbf{v}_{i_0}} \cdot \mathbf{v}_{i_0} > 0$, we have that, after unit replication, in the same direction ($\mathbf{v}_{i_0}^l = \mathbf{v}_{i_0}$):

$$\left. \frac{\partial \mathcal{L}(\mathbf{P})}{\partial s_{i_0}^l} \right|_{\mathbf{P}=\bar{\mathbf{P}}'} = \sum_{j \in J} \bar{h}_{ji_0} \mathbf{d}_{ji_0}^{\mathbf{v}_{i_0}^l} \cdot \mathbf{v}_{i_0}^l = \gamma_l \sum_{j \in J} \bar{h}_{ji_0} \mathbf{d}_{ji_0}^{\mathbf{v}_{i_0}} \cdot \mathbf{v}_{i_0} = \gamma_l \left. \frac{\partial \mathcal{L}(\mathbf{P})}{\partial s_{i_0}} \right|_{\mathbf{P}=\bar{\mathbf{P}}} \neq 0, \quad (26)$$

if $\gamma_l > 0, \forall l \in L$.

For any direction \mathbf{v}_{i_0} with $\left. \frac{\partial \mathcal{L}(\mathbf{P})}{\partial s_{i_0}} \right|_{\mathbf{P}=\bar{\mathbf{P}}} = \sum_{j \in J} \bar{h}_{ji_0} \mathbf{d}_{ji_0}^{\mathbf{v}_{i_0}} \cdot \mathbf{v}_{i_0} = 0$, we know that:

$$\mathbf{d}_{ji_0}^{\mathbf{v}_{i_0}} \cdot \mathbf{v}_{i_0} = 0, \quad \forall j \in J, \quad (27)$$

since the parameter before unit replication is a type-1 local minimum. After unit replication, we have that, in the same direction, in the same direction ($\mathbf{v}_{i_0}^l = \mathbf{v}_{i_0}$):

$$\left. \frac{\partial \mathcal{L}(\mathbf{P})}{\partial s_{i_0}^l} \right|_{\mathbf{P}=\bar{\mathbf{P}}'} = \sum_{j \in J} \bar{h}_{ji_0} \mathbf{d}_{ji_0}^{\mathbf{v}_{i_0}^l} \cdot \mathbf{v}_{i_0}^l = \gamma_l \sum_{j \in J} \bar{h}_{ji_0} \mathbf{d}_{ji_0}^{\mathbf{v}_{i_0}} \cdot \mathbf{v}_{i_0} = \gamma_l \left. \frac{\partial \mathcal{L}(\mathbf{P})}{\partial s_{i_0}} \right|_{\mathbf{P}=\bar{\mathbf{P}}} = 0, \quad (28)$$

and we also have:

$$\mathbf{d}_{ji_0}^{\mathbf{v}_{i_0}^l} \cdot \mathbf{v}_{i_0}^l = \mathbf{d}_{ji_0}^{\mathbf{v}_{i_0}} \cdot \mathbf{v}_{i_0} = 0, \quad \forall j \in J, \forall l \in L. \quad (29)$$

This shows that replicating with active propagation also avoids introducing escape neurons.

Thus, a unit replication strategy according to at least one of the two methods mentioned above is sufficient to avoid generating escape neurons.

■ **Necessary:**

We conduct this proof by contradiction. If we replicate a hidden neuron i_0 that is not tangentially flat (described by Equation (25)) with $\gamma_l = 0$ for some $l \in L$, we can prove that there must exist escape neurons in the resulting parameters. For convenience, let us specify that \hat{l} has $\gamma_{\hat{l}} = 0$.

Since Equation (25) holds, we can find a direction, denoted by a unit vector $\hat{\mathbf{v}}_{i_0}$, satisfying $\hat{\mathbf{v}}_{i_0} \cdot \bar{\mathbf{w}}_{i_0} = 0$ and $\left. \frac{\partial \mathcal{L}(\mathbf{P})}{\partial s_{i_0}} \right|_{\mathbf{P}=\bar{\mathbf{P}}} = \sum_{j \in J} \bar{h}_{ji_0} \mathbf{d}_{ji_0}^{\mathbf{v}_{i_0}} \cdot \hat{\mathbf{v}}_{i_0} > 0$, this must mean that there exists \hat{j} with:

$$\mathbf{d}_{\hat{j}i_0}^{\mathbf{v}_{i_0}} \cdot \hat{\mathbf{v}}_{i_0} \neq 0. \quad (30)$$

After unit replication, we have that, for the hidden neuron $i_0^{\hat{l}}$, the loss function's derivative with respect to its input weight in the direction of $\hat{\mathbf{v}}_{i_0^{\hat{l}}} = \hat{\mathbf{v}}_{i_0}$ is:

$$\left. \frac{\partial \mathcal{L}(\mathbf{P})}{\partial s_{i_0^{\hat{l}}}} \right|_{\mathbf{P}=\bar{\mathbf{P}}} = \sum_{j \in J} \bar{h}_{ji_0^{\hat{l}}} \mathbf{d}_{ji_0^{\hat{l}}}^{\mathbf{v}} \cdot \hat{\mathbf{v}}_{i_0^{\hat{l}}} = \gamma_{\hat{l}} \sum_{j \in J} \bar{h}_{ji_0} \mathbf{d}_{ji_0}^{\mathbf{v}_{i_0}} \cdot \hat{\mathbf{v}}_{i_0} = 0. \quad (31)$$

Additionally, we also have:

$$\mathbf{d}_{\hat{j}i_0^{\hat{l}}}^{\mathbf{v}} \cdot \hat{\mathbf{v}}_{i_0^{\hat{l}}} = \mathbf{d}_{\hat{j}i_0}^{\mathbf{v}_{i_0}} \cdot \hat{\mathbf{v}}_{i_0} \neq 0. \quad (32)$$

Equation (31) and (32) signifies the existence of one escape neuron $i_0^{\hat{l}}$ after unit replication. □

H.2.2 Preserving Stationarity Conditions

Lemma 4.8 is the sufficient and necessary conditions for preserving conditions for stationarity during unit replication. Proposition H.2.1.

H.3 Putting Things Together

We want to avoid generating escape neurons while preserving conditions for stationarity at the same time. The necessary and sufficient condition for the occurrence of these two events should be the intersection of the necessary and sufficient conditions in Proposition H.2.1 and Lemma 4.8, which is exactly the necessary and sufficient condition of Lemma 4.8.

I Results Regarding Inactive Units

There are 2 types of inactive units, depicted in Figure 11:

(2-1) *Orthogonal units*⁵

Add more hidden neurons, which are indexed with $i^0 \in I^0$, where h_{ji^0} is arbitrary, and $\mathbf{w}_{i^0} \cdot \mathbf{x}_k = 0$, for all $k \in K$.

(2-2) *Negative (positive) units.*

Suppose $\alpha^- = 0$. Add new hidden neurons $i^- \in I^-$, where $\mathbf{w}_{i^-} \cdot \mathbf{x}_k < 0$ for all $k \in K$, and h_{ji^-} are arbitrary for all $j \in J$. This is what we call negative units. This embedding scheme can likewise be extrapolated for when $\alpha^+ = 0$, giving positive units.

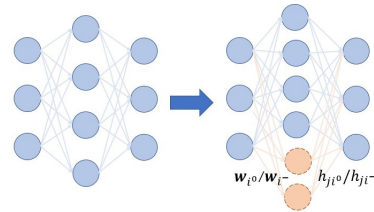


Figure 11: inactive units

I.1 Results Regarding Orthogonal Units

This type of network embedding does not generally preserve conditions for stationarity or local minimality. Nonetheless, based on our definition of stationary points in Section 3.2 and our analysis of local minima in Section 4.1, one can carry out investigations into them on a case-by-case basis when analyzing a specific example.

Let us first discuss whether stationarity will be preserved under this network embedding scheme. Let us denote the parameters after adding orthogonal units by \mathbf{P}' . Since the newly added hidden neurons satisfy $\mathbf{w}_{i^0} \cdot \mathbf{x}_k = 0$ for all $k \in K$, we know that $\left. \frac{\partial \mathcal{L}(\mathbf{P})}{\partial h_{ji^0}} \right|_{\mathbf{P}=\mathbf{P}'} = 0$, and $\left. \frac{\partial \mathcal{L}(\mathbf{P})}{\partial r_{i^0}} \right|_{\mathbf{P}=\mathbf{P}'} = 0$.

⁵Orthogonal units are not discussed in [8].

Thus, whether the tangential derivative preserves the condition in Definition 3.3 determines whether stationarity is preserved. For the tangential derivative, we have:

$$\left. \frac{\partial \mathcal{L}(\mathbf{P})}{\partial s_{i^0}} \right|_{\mathbf{P}=\mathbf{P}'} = \sum_{j \in J} h_{ji^0} \mathbf{d}_{ji^0}^{\mathbf{v}_{i^0}} \cdot \mathbf{v}_{i^0}. \quad (33)$$

Stationarity would require the above to be non-negative for all possible tangential direction \mathbf{v}_{i^0} , which cannot be guaranteed for general cases. Certain trivial cases where definite conclusions can be established are when the network has reached zero loss ($\mathbf{d}_{i^0}^{\mathbf{v}_{i^0}} = 0$ for all possible \mathbf{v}_{i^0}) or $h_{ji^0} = 0$ for all $j \in J$. In those cases, stationarity will be preserved.

We are not able to have general conclusions regarding whether the insertion of orthogonal units preserves type-1 local minimality as well since orthogonal units do not specify anything regarding whether they are escape neurons in general.

I.2 Results Regarding Negative Units

Proposition I.1. *Suppose that $\alpha^- = 0$. Adding **negative units** preserves the stationarity of stationary points.*

Proof. Let us denote the parameters after the insertion of negative units by $\bar{\mathbf{P}}'$. It is easy to check that the parameters associated with the originally existing hidden neurons $i \in I$ still satisfy the conditions for stationarity after inserting the negative units, since the negative units do not change the network output y_k for all inputs \mathbf{x}_k . For the negative units $i^- \in I^-$, we observe the following.

$$\mathbf{d}_{ji^-} = \sum_{\substack{k: \\ \mathbf{w}_{i^-} \cdot \mathbf{x}_k > 0}} \alpha^+ e_{kj} \mathbf{x}_k = 0, \quad (34)$$

since this summation will be over an empty set of k . This leads to $\left. \frac{\partial \mathcal{L}(\mathbf{P})}{\partial h_{ji^-}} \right|_{\mathbf{P}=\bar{\mathbf{P}}'} = 0$ and $\left. \frac{\partial \mathcal{L}(\mathbf{P})}{\partial r_{i^-}} \right|_{\mathbf{P}=\bar{\mathbf{P}}'} = 0$ according to their formulae in Equation (3) and (4).

Moreover, we have $\mathbf{d}_{ji^-}^{\mathbf{v}_{i^-}} = \mathbf{d}_{ji^-}$ for tangential direction \mathbf{v}_{i^-} of \mathbf{w}_{i^-} , since \mathbf{w}_{i^-} is orthogonal to no \mathbf{x}_k 's. This shows that the tangential derivative of the loss function with respect to \mathbf{w}_{i^-} is also zero, according to Equation 5. □

Remark I.2. We remind the readers that [8] has already proved that adding negative units will preserve the local minimality of the network.

J Results Regarding Inactive Propagation

Inactive propagation can be carried out as shown in Figure 12: add hidden neurons $i^\times \in I^\times$, where \mathbf{w}_{i^\times} is taken arbitrarily and $h_{ji^\times} = 0, \forall j \in J$, as shown in Figure 12.

This type of network embedding also does not preserve stationarity or type-1 local minimality generally.

We start by discussing the preservation of stationarity. Let us denote the parameters after adding units with inactive propagation by \mathbf{P}' . In this case, the added hidden neurons have $h_{ji^\times} = 0$ for all $j \in J$. As a result, according to Equation 4 and Equation 5, the radial derivative (which exists only when $\mathbf{w}_{i^\times} \neq 0$) and tangential derivatives (towards all tangential directions) must all be zero. However, the derivative with respect to output weight might not be zero:

$$\left. \frac{\partial \mathcal{L}(\mathbf{P})}{\partial h_{ji^\times}} \right|_{\mathbf{P}=\mathbf{P}'} = \mathbf{w}_{i^\times} \cdot \mathbf{d}_{ji^\times}. \quad (35)$$

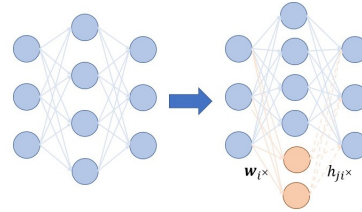


Figure 12: inactive propagation

Thus, the stationarity condition is not guaranteed to hold in general after adding inactive propagation units.

However, one may also notice that there are certain ways of enforcing stationarity: If we choose $\mathbf{w}_{i\times} = \mathbf{0}$ or $\mathbf{w}_{i\times} = \beta \mathbf{w}_i$ with $i \in I$, $\beta > 0$, then we equate Equation (35) to zero and preserves stationarity. The former also belongs to the case of orthogonal units, and the latter also belongs to the case of unit replication.

Then, we discuss whether type-1 local minimality is preserved. Preserving type-1 local minimality entails preserving stationarity and avoiding escape neurons, according to Theorem 4.2. We have discussed in the above that stationarity is not necessarily preserved in general. Moreover, regarding escape neurons, one can find that since an inactive propagation unit must have their tangential derivative being zero (since $h_{ji\times} = 0$), without further strong restriction on the $\mathbf{d}_{ji\times}$'s, the inactive propagation unit is highly possibly an escape neuron.

K Comparison of Theorem 10 of [8] and Lemma 4.8

[8] attempted to address the same question of whether local minimality is preserved by network embedding for our setup (which is also non-smooth) with its Theorem 10. It managed to find a specific scheme of unit replication that turns local minima into saddles, potentially contradicting Lemma 4.8. However, one can verify that the assumption in their theorem does not conform to our setting, which we explicate below.

Theorem 10 of [8] requires a constructed F matrix not to be a zero matrix to construct positive and negative eigenvalues for the Hessian matrix at the resulting parameters after unit replication. In this way, it is shown that the parameters after unit replication constitute a strict saddle. Please refer to [8] for more detail.

However, it turns out that, for the empirical squared loss, which is a widely used loss, the F matrix is zero at a type-1 local minimum, which we prove in the rest of this section. Hence Theorem 10 of [8] cannot say anything about such a situation.

Lemma K.1. *Suppose a set of parameters $\bar{\mathbf{P}}$ is a stationary point in our setting. If an input $\bar{\mathbf{w}}_i$ is such that $\mathbf{x}_k \cdot \bar{\mathbf{w}}_i \neq 0$, for all $k \in K$ (an assumption also taken by Theorem 10 of [8]), we must have that $\mathbf{d}_{ji} = \mathbf{0}$ for all $j \in J$.*

Proof. If $\mathbf{w}_i \cdot \mathbf{x}_k \neq 0$ for all $k \in K$, then the network is continuously differentiable. Thus we must have $\frac{\partial \mathcal{L}(\bar{\mathbf{P}})}{\partial s_i} = 0$ for all \mathbf{v}_i 's. Otherwise, it will not be a stationary point.

Moreover, the fact that the stationary point we are investigating is a type-1 local minimum gives:

$$\mathbf{d}_{ji} \cdot \mathbf{v}_i = \mathbf{d}_{ji}^{\mathbf{v}_i} \cdot \mathbf{v}_i = 0, \text{ for any tangential direction } \mathbf{v}_i \text{ of } \bar{\mathbf{w}}_i. \quad (36)$$

Moreover, since the parameter before unit replication $\bar{\mathbf{P}}$ is a stationary point, we must have:

$$\left. \frac{\partial \mathcal{L}(\mathbf{P})}{\partial h_{ji}} \right|_{\mathbf{P}=\bar{\mathbf{P}}} = \bar{\mathbf{w}}_i \cdot \mathbf{d}_{ji} = 0. \quad (37)$$

Thus, \mathbf{d}_{ji_0} must lie in the tangential space of $\bar{\mathbf{w}}_i$. If $\mathbf{d}_{ji_0} \neq \mathbf{0}$, then it must be parallel to some unit vector \mathbf{v}_i satisfying $\mathbf{v}_i \cdot \bar{\mathbf{w}}_i = 0$, which contradicts Equation (36). \square

Then we investigate the F matrix. It is helpful to recap the setting of adopted as the premise of Theorem 10 in [8]. First, they studied the ReLU activation function, meaning $\alpha^+ = 1, \alpha^- = 0$. Moreover, they only discussed replicating a hidden neuron i_0 with

$$\bar{\mathbf{w}}_{i_0} \cdot \mathbf{x}_k \neq 0, \forall k \in K, \quad (38)$$

which we account for in the above helper lemma. From [8], we know that $F \in \mathbb{R}^{d \times |J|}$ has each of its column being:

$$F_{:,j} = \sum_{k \in K} e_{kj} \frac{\partial \rho(\mathbf{x}_k \cdot \mathbf{w}_{i_0})}{\partial \mathbf{w}_{i_0}} = \sum_{\substack{k: \\ \mathbf{x}_k \cdot \mathbf{w}_{i_0} > 0}} e_{kj} \mathbf{x}_k = \mathbf{d}_{ji_0}. \quad (39)$$

Notice that the above derivative is not hindered by the non-differentiability in the activation function thanks to Equation (38).

Remember that we have proved $\mathbf{d}_{ji_0} = \mathbf{0}$ for all $j \in J$, rendering \mathbf{F} a zero matrix.

L Further Results Regarding the Numerical Experiments

L.1 The evolution of the learned function

In this section, we demonstrate the evolution of the learned function for both vanishing initialization and slightly larger initialization. We highlight the output function before and after the amplitude increase of the grouped living neurons.

The learned functions from vanishing initialization are shown in Figure 13. Remember that, to simulate vanishing initialization, we initialized all the parameters in the network independently with law $\mathcal{N}(0, (5 \times 10^{-6})^2)$. In Figure 13, we only draw the network function (using the blue line) with respect to the first component of the input, since the second component is always 1 in the training data to simulate the bias. Namely, in Figure 13, we draw the following function:

$$\tilde{y}(x) = \hat{y}((x, 1)), \quad x \in \mathbb{R}, \quad (40)$$

where $\hat{y}(\cdot)$ is the network function in Equation (1).

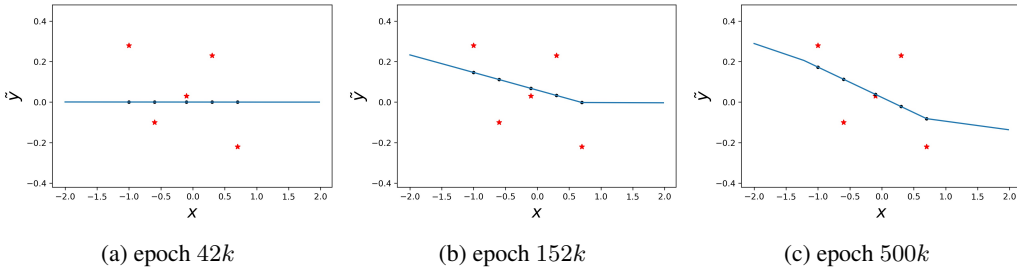


Figure 13: The evolution of the learned function during training with an initialization scale of 8×10^{-6} .

The five red stars are (x_k, y_k) 's, x_k 's being the first component of all the training samples, and y_k 's are the scalar target values. The five dots corresponds to $(x_k, \tilde{y}(x_k))$.

One can observe that, at epoch 42k, the network function is, approximately, a zero function. After the amplitude increase of the group 1 neurons, by epoch 152k, the network function has learned one kink. The amplitude increase starting from roughly epoch 152k forms the second kink of the network function. Afterward, the network stops evolving, keeping the two kinks before the end of training (epoch 500k).

The evolution of the learned function from a slightly larger initialization scale is shown in Figure 14. In this experiment, the parameters are initialized independently with law $\mathcal{N}(0, (8.75 \times 10^{-4})^2)$. We can observe that, with the amplitude increase of 4 groups of small living neurons at roughly epochs 14k, 66k, 144k, and 280k; there emerged 4 kinks. Notice, there should be 4 kinks in the learned function at the end. However, only 3 of them are shown, because the rest is located too far away from the input range we show in the image.

M Reproducibility

The code of the numerical experiments in this paper can be found at https://anonymous.4open.science/r/ReLU_like_loss_landscape-3B01/.

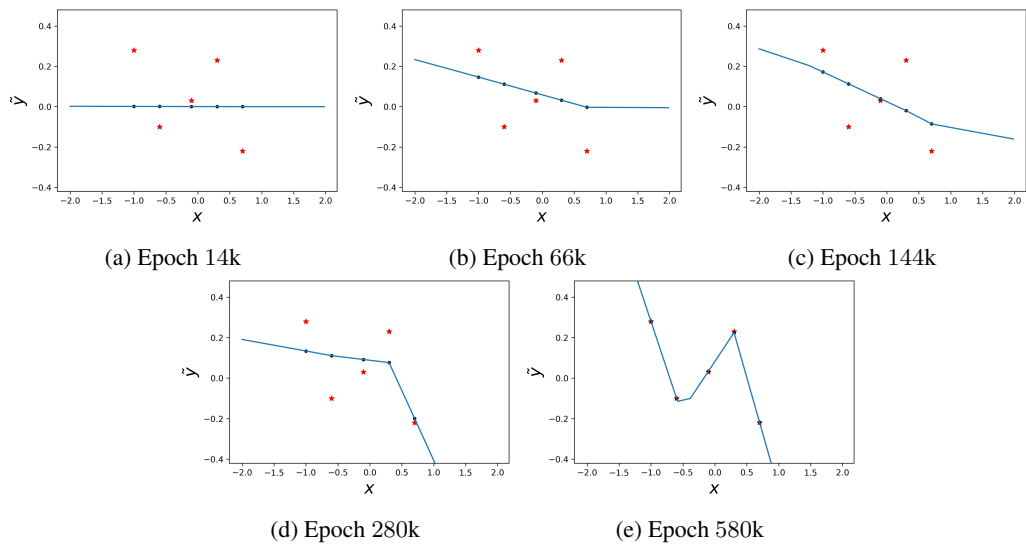


Figure 14: Evolution of the learned function during the training starting with a larger initialization scale.